Reliability-Based Semi-Analytical Solution for Ground Improvement by PVDs Incorporating Inherent (Spatial) Variability of Soil

Md. Wasiul Bari

Research Associate, Department of Civil Engineering,

Curtin University, WA 6845, Australia

E-mail: Md.Bari@curtin.edu.au

Mohamed A. Shahin†

Associate Professor, Department of Civil Engineering,

Curtin University, WA 6845, Australia

E-mail: M.Shahin@curtin.edu.au

†Corresponding author

Submitted to: **Computers and Geotechnics**

Reliability-Based Semi-Analytical Solution for Ground Improvement by PVDs Incorporating Inherent (Spatial) Variability of Soil

Md. Wasiul Bari and Mohamed A. Shahin

Abstract: The design of soil consolidation via prefabricated vertical drains (PVDs) has been traditionally carried out deterministically and thus can be misleading due to the ignorance of the uncertainty associated with the inherent (spatial) variation of soil properties. To treat such uncertainty in the design process of soil consolidation by PVDs, stochastic approaches that combine the finite element method with the Monte Carlo technique (FEMC) have been usually used. However, such approaches are complex, computationally intensive and time consuming. In this paper, a simpler reliability-based semi-analytical (RBSA) method is proposed as an alternative tool to the complex FEMC approach for soil consolidation by PVDs, considering soil spatial variability. The RBSA method is found to give similar results to those obtained from the FEMC approach and can thus be used with confidence in practice.

Keywords: Reliability-based design; Soil consolidation; Prefabricated vertical drains; Finite element method; Monte Carlo technique; Soil spatial variability.

1. Introduction

Traditionally, to predict soil consolidation by PVDs using available deterministic methods [e.g., 1, 2, 3], it has been usually assumed that the consolidating soil surrounding the

PVDs is homogeneous. In reality, however, the degree of consolidation achieved via PVDs is strongly dependent on soil properties that are spatially variable in nature, such as soil permeability, k, and volume compressibility, m_v. Consequently, the rate of soil consolidation is difficult to predict deterministically, especially for heterogeneous soil deposits. Therefore, it is crucial to develop more realistic solutions that can accommodate the true nature of the inherent (spatial) variability of soil in the course of design of soil consolidation by PVDs.

In recent years, a few attempts have been made to quantify and assess the uncertainty associated with soil consolidation. For example, some studies [i.e., 4, 5, 6] focussed on the impact of soil variability in one dimensional consolidation due to vertical drainage (i.e., no PVDs). A few more studies [i.e., 7, 8] focussed on the uncertainty associated with the measurement errors of soil testing for PVD-improved ground but soil spatial variability has not been explicitly investigated. More recently, Walker and Indraratna [9] proposed an analytical model incorporating a parabolic permeability distribution in the smear zone, and Basu et al. [10] performed a study to include a transition zone of linearly varying permeability between the smear and undisturbed zones with constant permeability. The above solutions, despite of being useful, failed to accommodate the true nature of soil spatial variability in design of ground improvement by PVDs and more alternative realistic solutions are needed.

In order to treat soil spatial variability in most geotechnical engineering problems, stochastic computational schemes that combine the finite element method and Monte Carlo technique [e.g., 6, 11, 12] have been often used. Despite the fact that such schemes offer successful solutions, they require a large number of simulations that are computationally intensive and time consuming. In the current study, an alternative simplified reliability-based semi-analytical (RBSA) approach is introduced for design of soil consolidation by PVDs, considering the spatial variations of soil permeability, k, and volume compressibility, m_v. The developed RBSA method is verified by comparing its results with those obtained from the complex stochastic 3D finite-element Monte-Carlo (FEMC) approach and the results are found to be in a good agreement. In the sections that follow, the stochastic FEMC approach is demonstrated first followed by detailed description of the alternative RBSA method.

2. Stochastic finite-element Monte-Carlo approach

For the purpose of examining the proposed RBSA method which will be discussed later in detail in the following section, a series of stochastic FEMC analyses are performed and their results are used for comparison with the RBSA method. The FEMC approach merges the local average subdivision (LAS) technique [13] and finite element (FE) modelling into a Monte Carlo framework using the following steps:

1. Identify the spatially variable soil properties affecting soil consolidation by PVDs;
2. Create a virtual soil profile that contains random fields of designated soil properties;
3. Incorporate the generated random fields of soil profile into FE modelling; and
4. Repeat Steps 2 and 3 many times using the Monte Carlo technique so that a series of consolidation responses is obtained from which probabilistic solution for soil consolidation can be derived.

The above steps, as well as the numerical procedures, are described below.

2.1 Identification of significant spatially variable soil properties

As indicated earlier, spatial variability of several soil properties can affect soil consolidation by PVDs. However, as confirmed by several researchers [e.g., 6, 14], soil permeability, k, and volume compressibility, $m_{v,}$ are the most significant factors affecting soil consolidation by PVDs. Although the coefficients of permeability in the vertical and horizontal directions (i.e., k_v and k_h, respectively) may vary in the ground, the impact of k_h is dominant [8]. Consequently, in the current study, only k_h and m_v are considered to be spatially variables, while the other soil properties are held constant and treated deterministically so as to reduce the superfluous complexity to the problem.

2.2 Generation of random fields of soil properties

In this study, the LAS method [13] extracted from the random field theory [15] are used to generate virtual random fields that allow rational random distributions of k_h and m_v, which are then implemented in the FEM modelling. Based on the random field theory, a random field of certain probability distribution of spatially variable soil property can be characterised by the soil property mean value, μ, variance, σ^2 (can also be represented by the standard deviation, σ, or coefficient of variation, υ, where $\upsilon = \sigma/\mu$) and correlation length or scale of fluctuation, θ. The value of θ describes the limits of spatial continuity and can simply be defined as the distance over which a soil property shows considerable correlation between two spatial points. Therefore, a large value of θ indicates strong correlation (i.e., uniform soil property field), whereas a small value of θ implies weak correlation (i.e., erratic soil property field).

In the current study, lognormally distributed random fields are assumed for simulating the spatial variability of k_h and m_v because this distribution is extensively used in the literature both for k_h and m_v [5, 6, 16]. To create a random field of soil property X, the following process is followed. A correlated local (arithmetic) average of normally distributed random field $G_X(i)$ over the domain of the ith element are first generated for 3D grid of soil mass with values of soil property of zero mean, unit variance and scale of fluctuation θ_X. The required lognormally distributed random field defined by μ_X and σ_X is then obtained using the following transformation function [17]:

$$X_i = \exp\{\mu_{\ln X} + \sigma_{\ln X} G_X(i)\} \tag{1}$$

where X_i is the soil property value assigned to the ith element; $\mu_{\ln X}$ and $\sigma_{\ln X}$ are, respectively, the mean and standard deviation of the underlying normally distributed ln(X) evaluated from the specified μ_X and σ_X of the lognormally distributed X as follows:

$$\mu_{\ln X} = \ln \mu_X - \frac{1}{2}\sigma^2_{\ln X} \tag{2}$$

$$\sigma_{\ln X} = \sqrt{\ln\left(1 + \frac{\sigma_X^2}{\mu_X^2}\right)} = \sqrt{\ln\left(1 + \upsilon_X^2\right)} \tag{3}$$

Rearranging Eqs. (2) and (3) gives the following inverse relationships for the mean and standard deviation of the lognormally distributed X:

$$\mu_X = \exp\left(\mu_{\ln X} + \frac{1}{2}\sigma^2_{\ln X}\right) \tag{4}$$

$$\sigma_X^2 = \mu_X^2\left(\exp\left(\sigma^2_{\ln X}\right) - 1\right) \tag{5}$$

The correlation coefficient for a soil property between two spatial points within the soil domain is specified by an exponentially decaying ellipsoidal Markov spatial correlation function, $\rho(\tau)$, as follows:

$$\rho(\tau) = \exp\left\{-\sqrt{\left(\frac{2\tau_x}{\theta_x}\right)^2 + \left(\frac{2\tau_y}{\theta_y}\right)^2 + \left(\frac{2\tau_z}{\theta_z}\right)^2}\right\} \tag{6}$$

where τ_x, τ_y and τ_z are, respectively, the distances between two points in x, y and z directions; and θ_x, θ_y and θ_z are, respectively, the scales of fluctuation in x, y and z directions. It should be noted that the spatial correlation function in Eq. (6) becomes statistically isotropic when θ_x = θ_y = θ_z. It is worthy to note that the scale of fluctuation is estimated with respect to the underlying normally distributed random field (i.e., ln$X$). Details on the estimation of the scale of fluctuation can be found in Lloret-Cabot et al. [18].

2.3 Finite element modelling incorporating soil spatial variability

The subsurface profile simulated in the previous step with the specified spatial variation of k_h and m_v can now be employed as inputs into a FE consolidation modelling of soil improvement by PVDs. In this study, all numerical analyses are carried out using a modified version of the FE computational scheme ‘‘Program 8.6’’ from the book by Smith and Griffiths [19] in which soil consolidation is treated as 3D uncoupled problem solved using implicit time integration with the ‘‘theta’’ method. The authors modified the source code of “Program 8.6” to incorporate the volume compressibility and allow for repetitive Monte-Carlo analyses.

To demonstrate the validity of the proposed RBSA method against the FEMC approach, a consolidation problem is considered for comparison implying a unit cell of soil with central cylindrical drain of dimensions L = 1.0m, r_e = 0.536m, r_s = 0.197m and r_w = 0.032m (see Fig. 1a). In the FE analyses, the circular influence area of the cylindrical unit cell is transformed to an equivalent square influence area (see Fig. 1b) of a side length $S = \sqrt{\pi r_e^2}$ (i.e., S = 0.95m). The selection of the equivalent square influence geometry in the FE modelling is convenient because it avoids the unfavourable mesh shape for the LAS method which requires square (or rectangular) elements to accurately compute locally averaged values of k_h and m_v for each element across the soil mass. For the same reason, a square shaped smear zone of side length S_s = 0.35m and PVD of a side length S_w = 0.05m are also employed in the FE modelling.

It is well known that the overall consolidation of PVD-improved ground is governed by the radial (horizontal) flow of water rather than the vertical flow as the drainage length in the horizontal direction is much less than that of the vertical direction and k_h is often much higher than that of k_v [2]. Under this reasoning, soil consolidation due to the horizontal drainage only is considered in the current study. Neglecting the vertical flow in the FE analyses is matched by setting k_v to be equal to zero and since the permeability variance is often described without referring to any direction, the two components of k_h (i.e., k_x and k_y) are assumed to be isotropic (i.e., $k_x = k_y = k_h$).

Although the accuracy of the FE solutions increases with the increase of the number of elements in the FE mesh, a trade-off between accuracy and run-time efficiency is necessary. Previous literature includes some recommendations regarding the optimum ratio of the scale of fluctuation to the finite element size. For example, Ching and Phoon [20] stated that this ratio should be ≥ 20, whereas Harada and Shinozuka [21] pointed out that it should be ≥ 2. In the current study, a sensitivity analysis on various FE mesh dimensions is conducted and it is found that a discretization of the FE mesh with an element of size 0.05m × 0.05m × 0.05m gives a reasonable precision and complies with the recommendation given by Harada and Shinozuka [21]. The 3D mesh used consists of 7220 eight node hexahedral elements (see Fig. 1b). The initial condition for the uncoupled analysis (i.e., no displacement degrees of freedom and only pore pressure degrees of freedom) is such that the excess pore pressure at all nodes (except at the nodes of the drain boundary) is set equal to 100 kPa, while the excess pore pressure at each node of the drain boundary is set equal to zero.

During the mandrel installation of PVDs, a disturbed zone surrounding the drain (i.e., smear zone) of reduced k_h and increased m_v is produced. However, soil spatial variability in the smear zone persists [22], albeit no longer fully natural. Under this reasoning, two groups of RBSA models are developed in this study under various assumed ground conditions. In the first group, the spatially variable soil properties are assumed to be continuous over the whole unit cell. However, non-stationary mean for the spatially variable soil properties are used to take into account the smear effect. In this case, the random fields of the spatially variable soil properties in the smear zone are generated separately from those of the undisturbed zone; however, this is carried out in such a way that the ratio of soil permeability in the undisturbed zone to the smear zone (i.e., k_h/k'_h) and the ratio of volume compressibility in the smear zone to the undisturbed zone (i.e., m'_v/m_v) are held constant. In the second group, it is assumed that the spatially variable soil properties in the smear zone are completely independent of those of the undisturbed zone. In this case, the random fields of the spatially variable soil properties for the undisturbed and smear zones are generated separately with their corresponding dimension and specified random field parameters. The well resistance is another factor that may affect the efficiency of PVD-improved ground, which is caused due to the deformation of the drain (i.e., folding, bending, crimping) and infiltration of fine soil particles through the drain filter. However, the discharge capacity of most available PVDs in the market is relatively high and well resistance can thus be practically ignored [23], which is the case in the presented example herein. It should be noted though that the proposed RBSA method can also take into account the well resistance effect, if needed.

In the current study, μ_{k_h} and μ_{m_v} are taken to be equal to 0.15m/year and 1.0×10^{-3}m^2/kN, respectively. The ratio $\mu_{k_h}/\mu_{k'_h}$, which may vary from 2 to 6 as reported by various researchers [e.g., 2, 23], is taken to be equal to 3. The ratio $\mu_{m'_v}/\mu_{m_v}$ is taken to be 1.2, which is in accordance with the value reported by Walker [24]. In order to validate the proposed RBSA, it is decided to conduct the study over the following range of υ and θ for k_h and m_v:

- υ_{k_h} (for both the smear and undisturbed zones) = 100, 200, 300 (%)
- υ_{m_v} (for both the smear and undisturbed zones) = 10, 20, 30 (%)
- $\theta_{k_h} = \theta_{m_v} = \theta$ (for both the smear and undisturbed zones) = 0.1, 0.25, 0.5, 1.0, 5.0, 10.0 (m)

It should be noted that the abovementioned selected ranges of υ and θ for k_h and m_v are typical to those reported in the literature [e.g., 25, 26] and are believed to represent sufficiently the practical values that can establish general trends for the stochastic soil consolidation behaviour. A single generation of the random fields and the subsequent FE analysis is termed "realization". For an individual realization, the degree of consolidation at any certain consolidation time, t, is expressed as $U(t)$ and can be calculated with the help of the following expression:

$$U(t) = 1 - \frac{\bar{u}(t)}{u_0} \tag{7}$$

where u_0 is the initial pore pressure and $\bar{u}(t)$ is the average pore pressures at any t (calculated by numerically integrating the excess pore pressure across the mesh and dividing by the total mesh volume), of the consolidation process.

2.4 Repetition of process based on the Monte Carlo technique

Following the procedures of the Monte Carlo technique, the process of generating random fields of k_h and m_v and the subsequent FE analysis is repeated numerous times with the same υ and θ until an acceptable accuracy of estimated statistics of $U(t)$ is achieved. It is found that 2000 Monte Carlo simulations are sufficient to yield reliable and reproducible estimates. One single case of FE analysis with 2000 Monte-Carlo simulations typically takes 6 days on an Intel core i5 CPU @ 3.4 GHz computer. The above repetitive process is performed for each combination of the selected υ and θ, and the obtained outputs from each realization of the Monte Carlo procedures are collated and statistically analyzed to make a comparative study between the FEMC approach and the proposed RBSA method, as will be seen later.

3. Reliability-based semi-analytical model

It is not uncommon that practicing engineers have neither the time nor the resources to perform full scale FEMC simulations of soil consolidation by PVDs including spatially random properties. Therefore, in this study, an approximate, easy to use reliability-based semi-analytical (RBSA) model is introduced from which direct estimates of the probability of achieving certain $U(t)$ can be readily obtained. The development of the RBSA model requires a performance function or a theoretical (deterministic) model as the commencing point to travel through to the reliability (stochastic) solution. Available deterministic analytical solutions for soil consolidation by PVDs are based on the unit cell concept for a single drain, which is also adopted in the RBSA model. It should be noted that the unit cell concept is deemed to be valid for stochastic analysis of PVD-improved ground because it was found in a recent study carried out by the authors using the FEMC approach that the multi-drain behaviour can be well represented by an idealized unit cell analysis, provided that certain factorized statistical parameters, computed by taking into account the size of the unit cell, are used so as to give equivalent solutions to those of the multi-drain. Detailed description of the validity of the unit cell concept for stochastic analyses of PVD-improved ground as compared to the multi-drain solution is beyond the scope of this paper and can be found elsewhere [see, 27].

In the current study, the commonly used radial consolidation equation of Hansbo [2] is used as the commencing point towards the RBSA model. This equation considers the unit cell concept and has gained a wide acceptance in practical application. The solution is based on the equal strain hypothesis and can estimate the degree of consolidation due to the horizontal drainage, $U_h(t)$, at any time, t, as given in the following equation (note that as the vertical flow is ignored in the FE solution, $U_h(t)$ from Hansbo's theory will be equal to $U(t)$ of the FE analysis and can be simply denoted as $U(t)$).

$$U(t) = 1 - \exp\left(-\frac{2k_h t}{m_v \gamma_w r_e^2 \alpha}\right) \tag{8}$$

$$\alpha = F_n + F_s + F_r \tag{9}$$

where F_n, F_s and F_r are the drain spacing factor, smear factor and well-resistance factor, respectively, and can be determined by:

$$F_n = \frac{n^2}{(n^2-1)}\left[\ln(n) - \frac{3}{4} + \frac{1}{n^2} - \frac{1}{4n^2}\right] \approx \ln(n) - \frac{3}{4} \tag{10}$$

$$F_s = \left(\frac{k_h}{k_h'} - 1\right)\ln\left(\frac{r_s}{r_w}\right) = \left(\frac{k_h}{k_h'} - 1\right)\ln(s) \tag{11}$$

$$F_r = \pi z(2L - z)\frac{k_h}{q_w} \tag{12}$$

where γ_w is the unit weight of water; r_e is the radius of the equivalent soil cylinder with impermeable perimeter (or the radius of zone of influence); t is the consolidation time; α is a group parameter representing the smear effect and geometry of the PVD system; $n = r_e/r_w$ is the drain spacing ratio (r_w is the equivalent radius of the drain); $s = r_s/r_w$ is the smear ratio (r_s is the radius of the smear zone); k_h' is the horizontal permeability of the smear zone; q_w is the vertical discharge capacity of the drain; L is the maximum vertical drainage distance; and z is the depth from the top of the consolidating layer. All parameters shown in Eqs. (8–12) are illustrated in Fig. 1.

It is mentioned earlier that the installation procedure of PVDs not only reduces k_h but also increases m_v within the smear zone, leading to different volume compressibility in the smear zone that is denoted earlier as m_v'. The ignorance of the increased m_v in the smear zone may lead to a lack of precision in the analysis. However, α parameter in Eq. (8) proposed by

Hansbo [2] disregards m_v'. In an effort to rectify this situation, Walker [24] introduced a new parameter termed as the smear zone volume compressibility parameter, α_{m_v}, is included in Eq. (8) to take into account m_v'. For a single smear zone with constant increased volume compressibility, α_{m_v} is given by Walker [24] as follows:

$$\alpha_{m_v} = \frac{n^2 - s^2}{n^2 - 1} + \frac{s^2 - 1}{n^2 - 1}\frac{m_v'}{m_v} \tag{13}$$

By including α_{m_v} into Eq. (8), a modified form of this equation is thus:

$$U(t) = 1 - \exp\left(-\frac{2k_h t}{m_v \gamma_w r_e^2 \alpha \alpha_{m_v}}\right) \tag{14}$$

If the changes of m_v in the smear zone are not considered, then α_{m_v} in Eq. (14) will be equal to 1.0. That is, Eq. (14) will return back to its original form of Hansbo's [2] formula presented in Eq. (8). Since k_h and m_v are the only random variables, rearranging Eq. (14) and defining $\ln[1/\{1-U(t)\}]$ as $U^*(t)$ gives:

$$U^*(t) = \frac{2t}{r^2\gamma_w}\frac{k_h}{m_v \alpha \alpha_{m_v}} \tag{15}$$

The above conversion of Eq. (14) to Eq. (15) is necessary as it simplifies the process of obtaining a closed form solution for the mean and variance of the degree of consolidation function $U^*(t)$ directly from the statistically defined input data (i.e., mean and variance) of k_h and m_v.

The reliability-based solution requires determination of a reasonable probability distribution of $U^*(t)$, once found, the statistical parameters of the distribution of $U^*(t)$ can be estimated. In this regard, simple semi-analytical relationships are derived to aid the designer in estimating the statistical parameters of the distribution of $U^*(t)$ directly from the random field parameters. This involves considering an approximate model where the geometric averages of k_h and m_v (i.e., $\bar{k}_h$ and $\overline{m}_v$, respectively) over the influence zone surrounding the PVD are used in Eq. (15). If the consolidating soil domain surrounding the PVD is termed D and discretized into an assembly of non-overlapping rectangular (or square) elements, then $\bar{k}_h$ and $\overline{m}_v$ over D can be defined as:

$$\bar{k}_h = \left[\prod_{i=1}^{j} k_{h_i}\right]^{1/j} = \exp\left[\frac{1}{j}\sum_{i=1}^{j} \ln k_{h_i}\right] = \exp\left\{\mu_{\ln k_h} + \sigma_{\ln k_h} \overline{G}_{k_h}(D)\right\} \tag{16}$$

$$\overline{m}_v = \left[\prod_{i=1}^{j} m_{v_i}\right]^{1/j} = \exp\left[\frac{1}{j}\sum_{i=1}^{j} \ln m_{v_i}\right] = \exp\left\{\mu_{\ln m_v} + \sigma_{\ln m_v} \overline{G}_{m_v}(D)\right\} \tag{17}$$

where i = 1,2, …, j represents the element number, $\overline{G}_{k_h}(D)$ and $\overline{G}_{m_v}(D)$ are the arithmetic averages of $G_{k_h}(i)$ and $G_{m_v}(i)$, respectively, over the domain D. It should be noted that k_h and m_v are assumed to be uncorrelated in the proposed RBSA model, which is due to the lack of data available in the literature to identify the degree and nature of the cross-correlation between k and m_v. For the problem of one dimensional consolidation, Freeze [5] reported that non-zero cross-correlation between k and m_v has a minor impact on the stochastic results of soil consolidation. Prior to finding the distribution and statistical parameters of $U^*(t)$, a brief discussion in regard to the underlying equivalent normally distributed mean and variance of the lognormally distributed soil property X (i.e., $\mu_{\ln \bar{X}}$ and $\sigma^2_{\ln \bar{X}}$) is essential, as follows.

As mentioned earlier, the overall behaviour of PVD system is not governed by the soil properties at discrete points but rather by the average soil properties of the soil volume within the soil domain. For example, in a consolidating heterogeneous soil mass, high flow rates in some regions of high k are offset by lower flow rates in other regions of low k, meaning that the total flow from the vicinity of PVD is effectively an averaging process. Despite the fact that the input statistics (i.e., μ, σ and θ) characterizing the random soil property of interest is defined at the point level, soil properties are rarely measured at a point and most engineering measurements concerned with soil properties are performed on samples of some finite volume, thus actually locally averaged over the sample volume. In light of this, the flow of water through spatially variable soil into the drain is essentially a process governed by the locally averaged soil properties. The local averaging is performed on the underlying point distribution (i.e., normal distribution) of the soil property of interest, which will lead to a reduction in the underlying point variance but the underlying mean will not be affected. For the lognormal distribution, however, both the mean and variance will be reduced by the local averaging, as the mean of a lognormal distribution depends on both the mean and variance of the underlying normal distribution. On the basis of the above discussion, the locally averaged mean of the underlying equivalent log-soil property field (ln*X*), $\mu_{\ln \bar{X}}$, which is unaltered by the local averaging can be given by:

$$\mu_{\ln \bar{X}} = \mu_{\ln X} \tag{18}$$

Using Eqs. (2) and (3), $\mu_{\ln \bar{X}}$ can be expressed in terms of the input statistics of *X*, as follows:

$$\mu_{\ln \bar{X}} = \mu_{\ln X} = \ln \mu_X - \frac{1}{2}\ln\left(1+\upsilon_X^2\right) \tag{19}$$

According to the local averaging theory [15], the variance, $\sigma^2_{\ln \bar{X}}$, which is affected by the local averaging, is given by:

$$\sigma^2_{\ln \bar{X}} = \gamma(D)\sigma^2_{\ln X} \tag{20}$$

where $\gamma(D)$ is the “variance function” that defines the amount by which the variance is reduced as a result of the local (arithmetic) averaging over a domain *D* and is a function of the size of the averaging domain and correlation function. The detailed calculation procedure of the variance reduction factor from the correlation function is given in Appendix A. It should be noted that, since the spatial variability of both k_h and m_v are modelled using 3D random fields and the FEMC results are obtained from 3D FEM analyses, $\gamma(D)$ in this study is also calculated using the 3D variance reduction function. By substituting Eq. (3) into Eq. (20), $\sigma^2_{\ln \bar{X}}$ can be expressed in terms of the prescribed statistics of X, as follows:

$$\sigma^2_{\ln \bar{X}} = \gamma(D)\ln\left(1+\upsilon_X^2\right) \tag{21}$$

For the purpose of comparing the proposed RBSA method with the FEMC approach, two groups of RBSA models are developed. The random soil properties are considered to be continuous over the whole unit cell in the first group, whereas random soil properties of the smear zone in the second group are assumed to be independent of the undisturbed zone. For each group, two RBSA models are developed to comply with the cases of considering both k_h and m_v as random variables, while only k_h is considered to be a random variable in the second case. For convenience, the RBSA models are denoted as G1C1 and G1C2 for the first group, whereas they are denoted as G2C1 and G2C2 for the second group. Considering the readership of the paper, only the two most general RBSA models, namely G1C1 and G2C2, are presented in th section below, whereas the other two RBSA models (i.e., G1C2 and G2C2) are presented in Appendix C. To facilitate the use of the RBSA models, an illustrated worked example will follow.

3.1 G1C1: RBSA model considering k_h and *m_v as continuous random variables over the entire unit cell*

In the development of the RBSA–G1C1 model, it is assumed that both k_h and m_v vary spatially in such a way that their second moment structures (variance, covariance, etc.) in the undisturbed and smear zones are identical with respect to the mean (i.e., $\upsilon_{k_k} = \upsilon_{k'_h}$, $\theta_{k_h} = \theta_{k'_h}$ and $\upsilon_{m_v} = \upsilon_{m'_v}$, $\theta_{m_v} = \theta_{m'_v}$). This means that the variance and covariance structure is assumed to be stationary. However, non-stationary means for k_h and m_v are used to take into account the smear effect. This is considered because non-stationary correlation structures are uncommon in geotechnical engineering due to the prohibitive volumes of data required to estimate their parameters. In geotechnical engineering, random-field models are often non-stationary in their mean; however, the variance and covariance structure is generally assumed to be stationary (Fenton and Griffiths 2008). As k_h and m_v are continuous over the entire soil domain, each point in the unit cell is correlated to each other. Therefore, it can be assumed that $\mu_{k_h} / \mu_{k'_h}$ and $\mu_{m'_v} / \mu_{m_v}$ remain constant in the unit cell. In other words, α and α_{m_v} contribute with little or no variability to $U^*(t)$. Considering k_h and m_v as the only random variables and using their geometric averages, Eq. (15) becomes:

$$U^*(t) = C \frac{\bar{k}_h}{\bar{m}_v} \tag{22}$$

where $\bar{k}_h$ and $\bar{m}_v$ are, respectively, the geometric averages of soil permeability and volume compressibility;

$$C = \frac{2t}{r_e^2 \gamma_w \alpha \alpha_{m_v}} \tag{23}$$

$$\alpha = \ln\left(\frac{n}{s}\right) - \frac{3}{4} + \frac{\mu_{k_h}}{\mu_{k'_h}} \ln(s) + F'_r \tag{24}$$

$$\alpha_{m_v} = \frac{n^2 - s^2}{n^2 - 1} + \frac{s^2 - 1}{n^2 - 1} \frac{\mu_{m'_v}}{\mu_{m_v}} \tag{25}$$

Since the random variation of well resistance effect is not considered in this study, F'_r in Eq. (24), which represents the average well resistance effect over the entire drain length, can be estimated as [28]:

$$F'_r = \frac{2\pi L^2}{3} \frac{\mu_{k_h}}{q_w} \tag{26}$$

Now a reasonable distribution for $U^*(t)$ can be found. Since both k_h and m_v are assumed to be lognormally distributed, then $\bar{k}_h$ and $\bar{m}_v$ are also lognormally distributed (based on the central limit theorem, the geometric average of a random variable tends to have a lognormal distribution), and therefore $U^*(t)$ will be lognormally distributed. In such a case, taking the logarithm of Eq. (22) yields:

$$\ln U^*(t) = \ln C + \ln \bar{k}_h - \ln \bar{m}_v \tag{27}$$

To evaluate the probability of achieving a certain $U(t)$, the mean $\mu_{\ln U^*(t)}$ and variance $\sigma^2_{\ln U^*(t)}$ of $\ln U^*(t)$ need to be estimated. The mean $\mu_{\ln U^*(t)}$ of $\ln U^*(t)$ can be obtained by taking the expectation of Eq. (27), as follows:

$$\mu_{\ln U^*(t)} = \ln C + \mu_{\ln \bar{k}_h} - \mu_{\ln \bar{m}_v} \tag{28}$$

Assuming no cross-correlation between k_h and m_v, the variance $\sigma^2_{\ln U^*(t)}$ of $\ln U^*(t)$ can be simply estimated, as follows:

$$\sigma^2_{\ln U^*(t)} = \sigma^2_{\ln \bar{k}_h} + \sigma^2_{\ln \bar{m}_v} \tag{29}$$

The four unknown parameters: $\mu_{\ln \bar{k}_h}$, $\mu_{\ln \bar{m}_v}$, $\sigma^2_{\ln \bar{k}_h}$ and $\sigma^2_{\ln \bar{m}_v}$ in Eqs. (28) and (29) are now need to be expressed in terms of the known statistical input parameters of k_h and m_v. With reference to Eq. (19), the following expressions of $\mu_{\ln \bar{k}_h}$ and $\mu_{\ln \bar{m}_v}$ are obtained:

$$\mu_{\ln \bar{k}_h} = \mu_{\ln k_h} = \ln \mu_{k_h} - \frac{1}{2}\ln\left(1+\upsilon^2_{k_h}\right) \tag{30}$$

$$\mu_{\ln \bar{m}_v} = \mu_{\ln m_v} = \ln \mu_{m_v} - \frac{1}{2}\ln\left(1+\upsilon^2_{m_v}\right) \tag{31}$$

With reference to Eq. (21), $\sigma^2_{\ln \bar{k}_h}$ and $\sigma^2_{\ln \bar{m}_v}$ can then be expressed with the specified statistical parameters of k_h and m_v, as follows:

$$\sigma^2_{\ln \bar{k}_h} = \gamma(D)_{k_h}\left(\ln\left(1+\upsilon^2_{k_h}\right)\right) \tag{32}$$

$$\sigma^2_{\ln \bar{m}_v} = \gamma(D)_{m_v}\left(\ln\left(1+\upsilon^2_{m_v}\right)\right) \tag{33}$$

where $\gamma(D)_{k_h}$ and $\gamma(D)_{m_v}$ are the variance reduction factors for k_h and m_v, respectively. As the inherent spatial variability of both k_h and m_v is pertinent over the whole unit cell, the entire soil domain, D, is used for estimating $\gamma(D)_{k_h}$ and $\gamma(D)_{m_v}$.

Now $\mu_{\ln U^*(t)}$ and $\sigma^2_{\ln U^*(t)}$ can be evaluated by substituting $\mu_{\ln \bar{k}_h}$ and $\mu_{\ln \bar{m}_v}$ in Eq. (28), and $\sigma^2_{\ln \bar{k}_h}$ and $\sigma^2_{\ln \bar{m}_v}$ in Eq. (29), as follows:

$$\mu_{\ln U^*(t)} = \ln C + \left[\ln \mu_{k_h} - \frac{1}{2}\ln\left(1+\upsilon^2_{k_h}\right)\right] - \left[\ln \mu_{m_v} - \frac{1}{2}\ln\left(1+\upsilon^2_{m_v}\right)\right] \tag{34}$$

$$\sigma^2_{\ln U^*(t)} = \gamma(D)_{k_h}\left(\ln\left(1+\upsilon^2_{k_h}\right)\right) + \gamma(D)_{m_v}\left(\ln\left(1+\upsilon^2_{m_v}\right)\right) \tag{35}$$

Using the developed semi-analytical relationships shown in Eqs. (34) and (35), the procedure for evaluating $\mu_{\ln U^*(t)}$ and $\sigma^2_{\ln U^*(t)}$ can then be summarized as follows:

1. Determine the mean, standard deviation and scale of fluctuation of k_h and m_v (i.e., μ_{k_h}, σ_{k_h} and θ_{k_h}; and μ_{m_v}, σ_{m_v} and θ_{m_v});
2. Calculate $\upsilon_{k_h} = \sigma_{k_h} / \mu_{k_h}$ and $\upsilon_{m_v} = \sigma_{m_v} / \mu_{m_v}$;
3. Evaluate all constant parameters involved in the RBSA method (i.e., α, α_{m_v}, C, $\gamma(D)_{k_h}$ and $\gamma(D)_{m_v}$); and
4. Estimate $\mu_{\ln U^*(t)}$ and $\sigma^2_{\ln U^*(t)}$ by substituting C, μ_{k_h}, μ_{m_v}, υ_{k_h} and υ_{m_v} in Eq. (34), and $\gamma(D)_{k_h}$, $\gamma(D)_{m_v}$, υ_{k_h} and υ_{m_v} in Eq. (35).

3.2 G2C1: RBSA model considering k_h, k'_h, m_v and m'_v as independent random variables

As k_h, k'_h, m_v and m'_v are independent random variables, α and α_{m_v} are no longer constant parameters. Eq. (15) is therefore becomes:

$$U^*(t) = C\frac{\bar{k}_h}{\overline{m}_v \overline{\alpha}\,\overline{\alpha}_{m_v}} \tag{36}$$

where

$$C = \frac{2t}{r_e^2 \gamma_w} \tag{37}$$

$\overline{\alpha}$ and $\overline{\alpha}_{m_v}$ are, respectively, the equivalent α and α_{m_v} parameters of the spatially variable soil and can be expressed by the following equations:

$$\overline{\alpha} = \ln\left(\frac{n}{s}\right) - \frac{3}{4} + \frac{\bar{k}_h}{\bar{k}'_h}\ln(s) + F'_r \tag{38}$$

$$\overline{\alpha}_{m_v} = \frac{n^2 - s^2}{n^2 - 1} + \frac{s^2 - 1}{n^2 - 1}\frac{\overline{m}_v}{\overline{m}'_v} \tag{39}$$

Assuming that: $\ln\left(\frac{n}{s}\right) - \frac{3}{4} + F'_r = a$; $\ln(s) = b$ and $\frac{\bar{k}_h}{\bar{k}'_h} = W$, Eq. (38) becomes:

$$\overline{\alpha} = a + bW \tag{40}$$

Similarly, by assuming $\frac{n^2 - s^2}{n^2 - 1} = g$; $\frac{s^2 - 1}{n^2 - 1} = h$ and $\frac{\overline{m}_v}{\overline{m}'_v} = V$, Eq. (39) becomes:

$$\overline{\alpha}_{m_v} = g + hV \tag{41}$$

The parameters α and α_{m_v} are respectively the function of permeability and volume compressibility. Therefore, $\overline{\alpha}$ and $\overline{\alpha}_{m_v}$, and in turn $U^*(t)$ will also be approximately lognormally distributed. In such a case, the mean $\mu_{\ln U^*(t)}$ of ln$U^*(t)$ can be obtained by taking logarithm and subsequent expectation of Eq. (36):

$$\mu_{\ln U^*(t)} = \ln C + \mu_{\ln \bar{k}_h} - \mu_{\ln \overline{m}_v} - \mu_{\ln \overline{\alpha}} - \mu_{\ln \overline{\alpha}_{m_v}} \tag{42}$$

The variance of k_h, k'_h, m_v and m'_v contribute to the variance of ln$U^*(t)$. As $\overline{\alpha}$ and $\overline{\alpha}_{m_v}$ involve k_h, k'_h, m_v and m'_v, then by assuming no cross-correlation between any of the random variables, the variance $\sigma^2_{\ln U^*(t)}$ of ln$U^*(t)$ is thus:

$$\sigma^2_{\ln U^*(t)} = \sigma^2_{\ln \bar{\alpha}} + \sigma^2_{\ln \bar{\alpha}_{m_v}} \tag{43}$$

In order to obtain $\mu_{\ln U^*(t)}$ and $\sigma^2_{\ln U^*(t)}$ in Eqs. (42) and (43) above, the six unknown parameters $\mu_{\ln \bar{k}_h}$, $\mu_{\ln \bar{m}_v}$, $\mu_{\ln \bar{\alpha}}$, $\mu_{\ln \bar{\alpha}_{m_v}}$, $\sigma^2_{\ln \bar{\alpha}}$ and $\sigma^2_{\ln \bar{\alpha}_{m_v}}$ must be obtained in terms of the known statistical input parameters of k_h, k'_h, m_v and m'_v. The formulations of all unknown parameters are presented in Appendix B, as they are large enough not to be included in the main text so as to avoid any possible disruption to the readership of the paper. At the end of Appendix B, a procedure for calculating these unknown parameters is summarised from which $\mu_{\ln U^*(t)}$ and $\sigma^2_{\ln U^*(t)}$ can be estimated by substituting them in Eqs. (42) and (43).

Having established with reasonable accuracy the distribution parameters of ln$U^*(t)$ for the RBSA method, the probabilities of achieving a target degree of consolidation at any specified time, $U_s(t)$, can be obtained from the following lognormal probability distribution transformation:

$$P[U^*(t) \geq U_s^*(t)] = 1 - \Phi\left(\frac{\ln U_s^*(t) - \mu_{\ln U^*(t)}}{\sigma_{\ln U^*(t)}}\right) \tag{44}$$

where: P [.] = probability of its argument, Φ(.) is the standard normal cumulative distribution function and $U_s^*(t)$ is the target $U^*(t)$ that needs to be achieved. Since $U^*(t)$ is a monotonically increasing function of $U(t)$, the following equation holds [29]:

$$P[U^*(t) \geq U_s^*(t)] = P[U(t) \geq U_s(t)] \tag{45}$$

Assuming the target degree of consolidation is 90% (i.e., $U_s(t) =$ 0.9) and denoting it as U_{90}, the probability of achieving U_{90} at any time, t, can be estimated as follows:

$$P[U(t) \geq U_{90}] = P[U^*(t) \geq 2.3026] = 1 - \Phi\left(\frac{\ln 2.3026 - \mu_{\ln U^*(t)}}{\sigma_{\ln U^*(t)}}\right) \tag{46}$$

Note that when $U_s(t) = U_{90} = 0.9$, then $U_s{*}(t) = \ln[1/(1–0.9)] = 2.3026$. In the following section, detailed comparison between the results obtained from the stochastic FEMC approach and proposed RBSA method is presented and discussed.

4. Comparison between finite-element Monte-Carlo approach and reliability-based semi-analytical method

In this section, a comparison between the proposed RBSA method and FEMC approach is demonstrated through an illustrative worked example. For brevity and because of the good agreement between the results of the four proposed RBSA models (i.e., G1C1, G1C2, G2C1 and G2C2) and their corresponding FEMC solutions, only G1C1 and G2C1 models are presented herein. It is to be reminded that k_h and m_v in G1C1model are considered as continuous random variables over the entire unit cell, whereas in G2C1 model k_h and m_v in the smear and undisturbed zones are considered to be independent random variables. Prior to comparison, the rationality of the assumption of lognormal distribution for $U{*}(t)$ under various assumed ground conditions is assessed through the frequency density plot of $U{*}(t)$ on the basis of 2000 realizations for each combination of the variability parameters υ and θ for the spatially variable soil properties at several different consolidation time. The chi-square goodness-of-fit tests for all cases are performed and yielded p-values between 0.15–0.96. Such high p-values indicate that there is a very little evidence in the simulated $U{*}(t)$ sample against the null hypothesis of the assumed lognormal distribution. By accepting the lognormal distribution, all subsequent statistics of the underlying normally distributed $\ln U{*}(t)$ are estimated by the method of moments from the suite of 2000 realizations using the following transformations:

$$\mu_{\ln U*(t)} = \frac{1}{n_{sim}} \sum_{i=1}^{n_{sim}} \ln U*_i\,(t) \tag{47}$$

$$\sigma_{\ln U^*(t)} = \sqrt{\frac{1}{n_{sim}-1}\sum_{i=1}^{n_{sim}}[\ln U^*_i\,(t) - \mu_{\ln U^*(t)}]^2} \tag{48}$$

where: $U^*_i(t)$ is the $U^*(t)$ from the ith realization (i = 1, 2, 3, …, n_{sim}) and n_{sim} is the total number of realizations (i.e., 2000).

4.1 FEMC approach versus RBSA-G1C1 model

The illustrative example used for comparison between the FEMC approach and RBSA-G1C1 model involves the same unit cell consolidation problem illustrated earlier (i.e., L = 1.0m, r_w = 0.032m, r_e = 0.536m, r_s = 0.197m, n = 16.75 and s = 6.156). The spatial variability of k_h and m_v is assumed to have μ_{k_h} = 0.15 m/year, k_h/k'_h = 3.0, μ_{m_v} = 1.0×10^{-3} m^2/kN, m'_v/m_v = 1.2, $\upsilon_{k_h} = 200\,\%$, $\upsilon_{m_v} = 20\,\%$ and $\theta_{k_h} = \theta_{m_v}$ = 1.0m. Armed with the above information, $\mu_{\ln U^*(t)}$ (see Eq. (34)) and $\sigma^2_{\ln U^*(t)}$ (see Eq. (35)) are calculated by following the steps described earlier in developing the RBSA-G1C1 model, as explained below.

Since no well resistance is considered, the constant parameters involved in the RBSA method can be calculated using the following equations:

$$\alpha = \ln(16.75) - 075 + (3-1)\times\ln(6.156) = 5.703$$

$$\alpha_{m_v} = \frac{16.75^2 - 6.156^2}{16.75^2 - 1} + \frac{6.156^2 - 1}{16.75^2 - 1}\times 1.2 = 1.026$$

If the probability of achieving 90% consolidation is to be determined at 0.75 year, then the parameter C will be:

$$C = \frac{2\times 0.75}{0.536^2 \times 9.8 \times 5.703 \times 1.026} = 0.091 \text{ m year/kN}$$

Now using the algorithm presented in Appendix A, the variance reduction factor for k_h and m_v is given by:

$$\gamma(D)_{k_h} = \gamma(D)_{m_v} = \gamma(S, S, L) = 0.312$$

Substituting the given μ, υ and the calculated constant parameters in Eqs. (34) and (35) yield:

$$\mu_{\ln U^*(t)} = \ln(0.091) + [\ln 0.15 - 0.5\ln(1+2.0^2)] - [\ln 1.0\times 10^{-3} - 0.5\ln(1+0.2^2)] = 1.83$$

$\sigma^2_{\ln U^*(t)} = 0.312 \times \ln(1+2.0^2) + 0.312 \times \ln(1+0.2^2) = 0.514$, therefore, $\sigma_{\ln U^*(t)} = 0.717$

Using the computed values of $\mu_{\ln U^*(t)}$ and $\sigma_{\ln U^*(t)}$ in Eq. (46), the probability of achieving 90% consolidation from the RBSA–G2C1 model can be computed as follows:

$$P[U(t=0.75) \geq U_{90}] = 1 - \Phi\left(\frac{\ln(2.3026) - 1.83}{0.717}\right) = 0.92$$

The FEMC approach of the above problem yields $P[U(t=0.75) \geq U_{90}] = 0.94$, thus demonstrating an excellent agreement between the FEMC approach and proposed RBSA–G2C1 method. Following the above procedure, $\mu_{\ln U^*}$, $\sigma_{\ln U^*}$ and $P[U \geq U_{90}]$ at each time step over each combinations of the spatial variability parameters are evaluated for both solution approaches and the results are compared in Figs. 2–3. It should be noted that, for brevity, the results of only a few tests are presented.

The agreement between $\mu_{\ln U^*}$ and $\sigma_{\ln U^*}$ derived from the FEMC simulation and predicted by the RBSA-G1C1 model is examined in Fig. 2. The influence of υ on $\mu_{\ln U^*}$ is illustrated in Fig. 2(a) for a constant θ = 0.5m. It can be seen that, in general, the predicted values of $\mu_{\ln U^*}$ obtained from the RBSA model and the FEMC approach match exceptionally well. In both methods, the estimated $\mu_{\ln U^*}$ decreases with the increase of υ, as expected. The relationships between the estimated $\mu_{\ln U^*}$ versus the consolidation time, t, for various θ at constant $\upsilon_{k_h} = 200\,\%$ and $\upsilon_{m_v} = 20\,\%$ are shown in Fig. 2(b). It can be seen that the results obtained from both the FEMC approach and RBSA-G1C1 model are almost identical. In each solution method, even though the results for various θ are drawn in the plot, they are embodied into a single curve, implying that the obtained results at different θ are very close and cannot be distinguished. The virtually identical curves for all θ obtained from each method of analysis demonstrate that $\mu_{\ln U^*}$ is largely independent of θ. This is expected as in principle θ does not affect the local average mean of the normally distributed process.

The effect of υ on $\sigma_{\ln U^*}$ for a fixed value of θ = 0.5m is shown in Fig. 2(c), which shows that, in general, $\sigma_{\ln U^*}$ increases with the increase of υ and the agreement between the FEMC approach and RBSA model is very good. The influence of θ on $\sigma_{\ln U^*}$ at constant $\upsilon_{k_h} = 200\,\%$ and $\upsilon_{m_v} = 20\,\%$ is shown in Fig. 2(d). It can be seen that $\sigma_{\ln U^*}$ increases with the increase of θ for both approaches, and apart from some slight discrepancy at high $\theta \geq$ 5m, the agreement between the FEMC approach and RBSA model is reasonable and shows good compliance. This behaviour can be explained by noting that, when $\theta \rightarrow 0$, the simulated soil profile is consisted of an infinite number of independent 'observations', thus there is a decrease in the average variance of the consolidation rate and the averaging process almost perfectly predicts the condition in the unit cell. Conversely, when θ is large, the average variance of the consolidation rate is also expected to be large due to the decrease in the number of independent 'observations', resulting in less averaging variance reduction within each realization.

The agreement between the FEMC approach and RBSA-G1C1 model is examined in terms of $P[U \geq U_{90}]$ in Fig. 3. The effect of υ on $P[U \geq U_{90}]$ at a fixed value of θ = 0.5m is shown in Fig. 3(a). It can be seen that the two solutions are in a good agreement despite some slight discrepancy at the earlier stage of consolidation. This may be attributed to the fact that the FEMC approach relies on the free strain concept, while the RBSA method is based on Hansbo's solution of an equal strain assumption. As the probability of achieving a target degree of consolidation of usual interest is greater than 50%, any discrepancy in this range has a little implication from the practical point of view. In Fig. 3(b), the compliance between the FEMC approach and proposed RBSA method shows a good agreement for various θ at constant $\upsilon_{k_h} = 200\,\%$ and $\upsilon_{m_v} = 20\,\%$, although a slight discrepancy in $P[U \geq U_{90}]$ exists when θ is as small as 0.1m (i.e., for erratic soil). It can also be seen that for any $P[U \geq U_{90}] \geq$ 50%, the RBSA–G1C1 model yields slightly higher (unconservative) estimation of $P[U \geq U_{90}]$ than that calculated by the FEMC approach when θ is as low as 0.1m. On the other hand, $P[U \geq U_{90}]$ derived from the RBSA–G1C1 model is slightly lower (conservative) than those obtained from the FEMC approach when θ is as high as 1.0m.

4.2 FEMC approach versus RBSA–G2C1 model

Following the procedure set out in Appendix B, curves for $\mu_{\ln U^*}, \sigma_{\ln U^*}$ and in turn $P[U \geq U_{90}]$ with time over some selected combinations of the spatial variability parameters are obtained for RBSA-G2C1 method. The agreement between $\mu_{\ln U^*}$, $\sigma_{\ln U^*}$ and $P[U \geq U_{90}]$ derived from the FEMC simulation and predicted by the RBSA–G2C1 model are then examined in Figs. 4–9. As mentioned earlier, two independent random fields for k_h and m_v are generated for the undisturbed and smear zones. For convenience of presentation, the statistical parameters in the smear and undisturbed zones (i.e., υ and θ of k_h and m_v) are denoted with appropriate subscripts "*s*" and "*u*" depending on whether they are specified for the smear zone or undisturbed zone, where *s* refers to the smear zone while *u* refers to the undisturbed zone.

The influence of increasing υ on the agreement between the FEMC approach and RBSA–G2C1 model in terms of $\mu_{\ln U^*}$ at a fixed value of $\theta_u = \theta_s$ = 1.0m is shown in Fig. 4. It can be seen that, in general, the predicted values of $\mu_{\ln U^*}$ obtained from the RBSA model match those obtained from the FEMC approach reasonably well. In both methods, the estimated $\mu_{\ln U^*}$ decreases with the increase of υ, as expected. However, the identical curves for all cases of υ_u ($\upsilon_{k_h'}$ and $\upsilon_{m_v'}$ are fixed at 100% and 10%, respectively) for both methods in Fig. 4(a) indicate that the effect of increasing υ_u on $\mu_{\ln U^*}$ remains marginal. The effect of υ_s on $\mu_{\ln U^*}$ at fixed values of υ_{k_h} = 100% and υ_{m_v} = 10% is illustrated in Fig. 4(b). It can be seen that, although the agreement between the RBSA–G2C1 model and the FEMC approach is reasonably well, the discrepancy in $\mu_{\ln U^*}$ between the two methods becomes higher as t increases. Fig. 4 also demonstrates that the decreasing rate of $\mu_{\ln U^*}$ is higher for an increase in υ_s than υ_u.

The matching of $\mu_{\ln U^*}$ obtained from the RBSA-G2C1 model and FEMC approach is examined in Fig. 5 for an increasing θ at constant values of $\upsilon_{k_k} = \upsilon_{k'_h}$ = 200% and $\upsilon_{m_v} = \upsilon_{m'_v}$ = 20%. The effect of θ_u on $\mu_{\ln U^*}$ for a constant value of θ_s = 0.25m is shown Fig. 5(a), whereas the effect of θ_s on $\mu_{\ln U^*}$ for a fixed value of θ_u = 0.25m is shown in Fig. 5(b). It can be seen that the results obtained from both the FEMC approach and RBSA–G2C1 model are nearly identical. However, a slight discrepancy in $\mu_{\ln U^*}$ from the two solution approaches is found when the consolidation time t is as large as 1 year. In each solution method, the single curve for all θ confirms that $\mu_{\ln U^*}$ is independent of θ.

The agreement between the FEMC approach and RBSA–G2C1 model is further illustrated by matching the estimated $\sigma_{\ln U^*}$ at different values of υ_u and υ_s, and at a constant $\theta_u = \theta_s$ = 1.0m (see Fig. 6). It can be seen that, in general, $\sigma_{\ln U^*}$ increases with the increase of υ and the agreement between the two solution approaches is reasonably well. However, for a certain υ at any particular consolidation time t, the estimated values of $\sigma_{\ln U^*}$ derived from the RBSA–G2C1 model are slightly higher than those obtained from the FEMC approach. The above observation is more accurate for υ_s (see Fig. 6(b)) than υ_u (see Fig. 6(a)). The comparison shown in Fig. 6 reveals that $\sigma_{\ln U^*}$ is largely insensitive to varying υ_u and highly sensitive to increasing υ_s.

The effect of θ derived from the FEMC approach and RBSA–G2C1 model in terms of $\sigma_{\ln U^*}$ for fixed values of $\upsilon_{k_k} = \upsilon_{k'_h}$ = 200% and $\upsilon_{m_v} = \upsilon_{m'_v}$ = 20% is demonstrated in Fig. 7. It can be seen that $\sigma_{\ln U^*}$ increases with the increase of θ, and apart from some slight discrepancy at large θ (i.e., at $\theta \geq 5.0$m), the agreement between the two methods is again reasonably well. In

Fig. 7(a), it can be seen that varying θ_u (θ_s is fixed at 0.25m) has a marginal effect on $\sigma_{\ln U}$, while varying θ_s has a considerable impact on the estimated values of $\sigma_{\ln U*}$ (see Fig. 7(b)).

The influence of υ on the agreement between the FEMC approach and RBSA–G2C1 model in terms of $P[U \geq U_{90}]$ at a fixed value of $\theta_u = \theta_s$ = 1.0m is shown in Fig. 8. The effect of increasing υ_u on $P[U \geq U_{90}]$ is illustrated in Fig. 8(a). It can be seen that the predicted $P[U \geq U_{90}]$ obtained from the proposed RBSA–G2C1 model agrees exceptionally well with those obtained from the FEMC approach for all cases of υ_u ($\upsilon_{k'_h}$ and $\upsilon_{m'_v}$ are fixed at 100% and 10%, respectively). The virtually identical curves of $P[U \geq U_{90}]$ in Fig. 8(a) for all υ_u indicate that $P[U \geq U_{90}]$ is largely independent of υ_u. Fig. 8(b) illustrates the effect of υ_s on $P[U \geq U_{90}]$ at a fixed value of $\theta_u = \theta_s$ =1.0m. Although the overall agreement between the estimated $P[U \geq U_{90}]$ by the two methods is very good, the caveat, however, is that the RBSA–G2C1 model gives slightly unconservative estimate of $P[U \geq U_{90}]$ for any $P[U \geq U_{90}] > 50\%$ and particularly when $\upsilon_{k'_h} \geq 200\%$ with $\upsilon_{m'_v} \geq 20\%$. This higher values of predicted $P[U \geq U_{90}]$ given by the RBSA–G2C1 model is due to the higher predicted $\mu_{\ln U*}$, as shown in Fig. 4(b). Fig. 8 also illustrates that the increasing rate of $P[U \geq U_{90}]$ with respect to t decreases as υ increases and this effect is more pronounced for an increase in υ_s than υ_u.

Apart from some slight discrepancy particularly when $P[U \geq U_{90}]$ in the range between 70% − 90%, the FEMC approach and proposed RBSA–G2C1 model show good agreement for various θ_u (see Fig. 9(a)) and θ_s (see Fig. 9(b)) at constant values of υ_k = 100% and υ_{m_v} = 25% as illustrated in Fig 9. This discrepancy between the two solutions is expected because of the fact that the variability in $U(t)$ is zero at the beginning of consolidation (i.e., at t= 0.0), and gradually increases with the increase in the consolidation time until it reaches a maximum value at certain intermediate t, then decreases with further increase in time until it approaches zero again after the full consolidation is occurred. It can be seen that for any $P[U \geq U_{90}] \geq$ 50%, the values of $P[U \geq U_{90}]$ derived from the RBSA–G2C1 model are slightly higher (unconservative) than those obtained from the FEMC approach when θ is as low as 0.25m, while this trend becomes opposite (conservative) when θ is as high as 1.0m. The comparison in Fig. 9(a & b) reveals that the effect of θ_s on $P[U \geq U_{90}]$ is more significant than θ_u.

The overall conclusion from the above comparison in Figs. 4–9 is that the RBSA-G2C1 model and FEMC approach agree reasonably well despite some discrepancies in the results of $\mu_{\ln U^*}$, $\sigma_{\ln U^*}$ and $P[U \geq U_{90}]$. This is attributed mostly to the empirical adjustment of the RSBA model which is necessary due to the fact that the sum of two lognormally distributed random variables does not have a simple closed form solution. In addition, for both solution methods it is found that the probabilistic behavior of soil consolidation is governed by the spatial variation of the soil properties of the smear zone. This behavior is expected because all expelled water from the PVD must pass through the smear zone.

5. Discussion

It is noteworthy that the agreement between the proposed RBSA method and FEMC approach shown above was examined for a consolidation problem of a soil layer having a thickness of 1m and isotropic scale of fluctuation. Therefore, to arrive at a general conclusion regarding the validity of the proposed RBSA method compared to the FEMC approach for thicker soil layers of anisotropic correlation structure, the comparison is also tested for a more practical example of a unit cell of thickness of geometry L = 4.25m, r_e = 0.48m, r_s = 0.197m and r_w = 0.032m, and parameters μ_{k_h} = 0.15m/year, k_h/k'_h = 3.0, μ_{m_v} = 1.0×10^{-3}m^2/kN and m'_v/m_v = 1.2. The 3D FE mesh of such problem consisted of 24,565 eight node hexahedral elements of size 0.05m × 0.05m × 0.05m. The FEMC approach of the problem needed an intensive computational time of 28 days to run 2000 realizations on an Intel core i5 CPU @ 3.4 GHz computer. Therefore, only two FEMC simulation tests, named as FEMC1 and

FEMC2, are performed considering anisotropic θ. FEMC1 and FEMC2 stand for comparison with RBSA–G1C1 and FEMC2 and RBSA–G2C1 models, respectively. For FEMC1 and its counterpart RBSA–G1C1 model, the random field parameters are assumed to be as follows: $\upsilon_{k_h} = 200\%$, $\upsilon_{m_v} = 20\%$, $\theta_x = \theta_y = 10.0\text{m}$ and $\theta_z = 1.0\text{m}$. For FEMC2 and its counterpart RBSA–G2C1model, the spatial variability of k_h and m_v is assumed to have υ_{k_k} = $\upsilon_{k'_h}$ = 200%, υ_{m_v} = $\upsilon_{m'_v}$ = 20%, $\theta_x = \theta_y = 10.0\text{m}$ and $\theta_z = 1.0\text{m}$. The same θ for k_h and m_v for the smear and undisturbed zones are used in this investigation. The computed $\mu_{\ln U^*(t)}$, $\sigma_{\ln U^*(t)}$ and $P[U \geq U_{90}]$ from the two methods are compared in Fig. 10. It can be seen that $\mu_{\ln U^*(t)}$ (Fig. 10a), $\sigma_{\ln U^*(t)}$ (Fig. 10b) and $P[U \geq U_{90}]$ (Fig. 10c) obtained from both the FEMC approach and RBSA method are almost identical, implying very good agreement between the two methods. This is due to the fact that the stochastic response of soil consolidation by PVDs is dependent on the ratio of the scale of fluctuation to the dimensions of the influence zone surrounding the PVD, which can be readily taken into account by the use of a variance reduction function. Therefore, the proposed RBSA method can be utilized with confidence as an easy-to-use alternative to the computationally intensive FEMC approach for assessing the reliability of soil consolidation by PVDs in spatially variable soils. Despite the fact that the proposed RBSA method is suitable for hand calculations, it is coded by the authors in FORTRAN to provide a user friendly executable program that can be readily used by practitioners, and the program is available for interested readers upon request.

6. Conclusions

Simple reliability-based semi-analytical (RBSA) models for predicting the statistics and probability of achieving a target degree of consolidation for PVD-improved ground were developed incorporating the inherent (spatial) variability of soils. The performance function of the proposed RBSA models was based on the well-known deterministic equation of Hansbo [2], which considers soil consolidation due to the horizontal drainage only. Under various ground conditions, the proposed RBSA models account for the spatial variability of soil volume compressibility and/or soil permeability, which are considered to be the most significant spatial random variables affecting soil consolidation by PVDs.

The results confirm that there is good agreement between the proposed RBSA method and the finite-element Monte-Carlo (FEMC) approach, implying that the simpler RBSA method negates the need for the computationally intensive and time consuming FEMC technique. The results also indicate that, for given coefficients of variation of soil permeability and volume compressibility, the stochastic response of soil consolidation by PVDs is dependent on the ratio of the scale of fluctuation to the dimensions of the influence zone surrounding the PVD, which can be readily taken into account by the use of a variance reduction function. Therefore, the proposed RBSA model can be confidently employed to assess the reliability of consolidation problems implying arbitrary dimensions.

Despite the success of the proposed RBSA method for design of PVD-improved ground, it has some limitations compared to the FEMC approach which can deal with more general cases and offers the ability to solve problems with less restrictive conditions. For example, the RBSA method does not consider soil consolidation due to the vertical drainage; hence, the computed probability of achieving a target degree of consolidation would be slightly conservative. However, it should be emphasised that, in practice, the contribution of soil consolidation due to the vertical drainage is only a small fraction of the overall soil consolidation and can thus be neglected without significant impact on the design results. In addition, soil permeability and volume compressibility were assumed to be uncorrelated, which again may lead to somewhat conservative solutions. However, it was reported by

Freeze [5] that the impact of non-zero correlation between k and m_v on problems of one dimensional consolidation is quite minor and the uncorrelated assumption adopted in the RBSA method is thus reasonable. The overall conclusion is that despite the abovementioned minor limitations of the proposed RBSA method compared to the FEMC approach, the RBSA provides more practical design for PVD-improved ground with an acceptable accuracy, which negates the need for the more sophisticated FEMC approach that requires impractical intensive computational time.

Appendix A. Variance reduction function

Considering the averaging domain D is a cube of dimension $X \times Y \times Z$, then $\gamma(D)$ corresponding to the Markov correlation function (see Eq. (6)) can be can be defined by Eq. (A.1), as follows [17]:

$$\gamma(X,Y,Z) = \frac{1}{X^2Y^2Z^2} \times \int_0^X \int_0^X \int_0^Y \int_0^Y \int_0^Z \int_0^Z \rho(\varsigma_1 - \xi_1, \varsigma_2 - \xi_2, \varsigma_3 - \xi_3) d\varsigma_1 d\xi_1 d\varsigma_2 d\xi_2 d\varsigma_3 d\xi_3 \quad \text{(A.1)}$$

The sixfold integration in Eq. (A.1) can be condensed to a threefold integration by taking advantage of the quadrant symmetry of the Eq. (6) as follows [17]:

$$\gamma(X,Y,Z) = \frac{8}{X^2Y^2Z^2} \times \int_0^X \int_0^Y \int_0^Z (X - \tau_1)(Y - \tau_2)(Z - \tau_3) \rho(\tau_1, \tau_2, \tau_3) d\tau_1 d\tau_2 d\tau_3 \quad \text{(A.2)}$$

Eq. (A.2) can be computed numerically with reasonable accuracy using Gaussian quadrature integration scheme as follows [17]:

$$\gamma(X,Y,Z) = \frac{1}{8} \sum_{i=1}^{n_g} \omega_i (1 - \psi_i) \sum_{j=1}^{n_g} \omega_j (1 - \psi_j) \sum_{k=1}^{n_g} \omega_k (1 - \psi_k) \rho(\varsigma_i, \xi_j, \vartheta_k) \quad \text{(A.3)}$$

where

$$\varsigma_i = X(1 + \psi_i)/2, \xi_j = Y(1 + \psi_j)/2, \vartheta_k = Z(1 + \psi_k)/2 \quad \text{(A.4)}$$

In which, ω_i, ϑ_i, and n_g are the weights, Gauss points, and their total number, respectively.

Appendix B. Computation of $\mu_{\ln\bar{k}_h}$, $\mu_{\ln\overline{m}_v}$, $\mu_{\ln\bar{\alpha}}$, $\mu_{\ln\bar{\alpha}_{m_v}}$, $\sigma^2_{\ln\bar{\alpha}}$ and $\sigma^2_{\ln\bar{\alpha}_{m_v}}$

With reference to Eqs. (18) and (19), $\mu_{\ln\bar{k}_h}$ and $\mu_{\ln\overline{m}_v}$ can be calculated as follows:

$$\mu_{\ln\bar{k}_h} = \mu_{\ln k_h} = \ln\mu_{k_h} - \frac{1}{2}\ln\left(1+\upsilon^2_{k_h}\right) \tag{B.1}$$

$$\mu_{\ln\overline{m}_v} = \mu_{\ln m_v} = \ln\mu_{m_v} - \frac{1}{2}\ln\left(1+\upsilon^2_{m_v}\right) \tag{B.2}$$

Taking expectation of Eqs. (40) and (41) yield the following equations of the mean of $\bar{\alpha}$ (i.e., $\mu_{\bar{\alpha}}$) and $\bar{\alpha}_{m_v}$ (i.e., $\mu_{\bar{\alpha}_{m_v}}$):

$$\mu_{\bar{\alpha}} = a + b\mu_W \tag{B.3}$$

$$\mu_{\bar{\alpha}_{m_v}} = g + h\mu_V \tag{B.4}$$

The variance of $\bar{\alpha}$ (i.e., $\sigma^2_{\bar{\alpha}}$) and $\bar{\alpha}_{m_v}$ (i.e., $\mu_{\bar{\alpha}_{m_v}}$) are thus:

$$\sigma^2_{\bar{\alpha}} = b^2\sigma^2_W \tag{B.5}$$

$$\sigma^2_{\bar{\alpha}_{m_v}} = h^2\sigma^2_V \tag{B.6}$$

Recalling that, $W = \bar{k}_h / \bar{k}'_h$ and $V = \overline{m}_v / \overline{m}'_v$. Since both $\bar{k}_h$, $\bar{k}'_h$, $\overline{m}_v$ and $\overline{m}'_v$ are lognormally distributed, W and V will also be approximately lognormally distributed. According to Eqs. (18) and (19), the following expressions of $\mu_{\ln W}$ and $\mu_{\ln V}$ with the known parameters are derived:

$$\mu_{\ln W} = \mu_{\ln\bar{k}_h} - \mu_{\ln\bar{k}'_h} = \left(\ln\mu_{k_h} - \frac{1}{2}\ln\left(1+\upsilon^2_{k_h}\right)\right) - \left(\ln\mu_{k'_h} - \frac{1}{2}\ln\left(1+\upsilon^2_{k'_h}\right)\right) \tag{B.7}$$

$$\mu_{\ln V} = \mu_{\ln\overline{m}'_v} - \mu_{\ln\overline{m}_v} = \left(\ln\mu_{m'_v} - \frac{1}{2}\ln\left(1+\upsilon^2_{m'_v}\right)\right) - \left(\ln\mu_{m_v} - \frac{1}{2}\ln\left(1+\upsilon^2_{m_v}\right)\right) \tag{B.8}$$

Since k_h and k'_h are independent random variables (no correlation between k_h and k'_h) and pertinent only over the undisturbed soil domain, D_u, and the smear zone, D_s, respectively, the overall variance $\sigma^2_{\ln W}$ of ln$W$ can be estimated with reference to Eqs. (20) and (21) as follows:

$$\sigma^2_{\ln W} = \frac{\left(\sigma^2_{\ln \bar{k}_h}\right) + \left(\sigma^2_{\ln \bar{k}'_h}\right)}{2} = \frac{\gamma(D_u)_{k_h}\ \ln\left(1+\upsilon^2_{k_h}\right) + \gamma(D_s)_{k'_h}\ \ln\left(1+\upsilon^2_{k'_h}\right)}{2} \tag{B.9}$$

and for the same reason,

$$\sigma^2_{\ln V} = \frac{\gamma(D_u)_{m_v}\ \ln\left(1+\upsilon^2_{m_v}\right) + \gamma(D_s)_{m'_v}\ \ln\left(1+\upsilon^2_{m'_v}\right)}{2} \tag{B.10}$$

where $\gamma(D_u)_{k_h}$, $\gamma(D_s)_{k'_h}$, $\gamma(D_u)_{m_v}$ and $\gamma(D_s)_{m'_v}$ are the variance reduction factors for k_h, k'_h, m_v and m'_v, respectively.

It can be noticed that both $\mu_{\ln W}$ and $\sigma^2_{\ln W}$ of underlying normally distributed ln$W$ are now known. So μ_W and σ^2_W of lognormally distributed W can readily be obtained with reference to Eqs. (4) and (5). However, as k_h and k'_h are not distributed over the entire soil domain and do not have the same influence on the overall behaviour of soil consolidation, the true μ_W and σ^2_W will be somewhat different from those calculated directly using $\mu_{\ln W}$ and $\sigma^2_{\ln W}$. For this reason, the expressions for μ_W and σ^2_W are empirically adjusted to obtain these two parameters of lognormally distributed W with reasonable accuracy as follows:

$$\mu_W = \left(\frac{2\mu_{\bar{k}_h}}{\mu_{\bar{k}_h} + \mu_{\bar{k}'_h}}\right)^{\chi} \exp\left(\mu_{\ln W} + \frac{1}{2}\sigma^2_{\ln W}\right) \tag{B.11}$$

where $\chi = \dfrac{\upsilon_{\bar{k}'_h}}{\upsilon_{\bar{k}_h}}$ if $\upsilon_{\bar{k}_h} > \upsilon_{\bar{k}'_h}$ and $\chi = \dfrac{\upsilon_{\bar{k}'_h} - \upsilon_{\bar{k}_h}}{\upsilon_{\bar{k}'_h}}$ if $\upsilon_{\bar{k}'_h} > \upsilon_{\bar{k}_h}$

$$\sigma^2_W = \left(\frac{2\upsilon_{\bar{k}'_h}}{\upsilon_{\bar{k}_h} + \upsilon_{\bar{k}'_h}}\right)\mu^2_W\left[\exp\left(\sigma^2_{\ln W}\right) - 1\right] \tag{B.12}$$

The reason as stated above for the empirical adjustment of μ_W and σ_W^2 is also applicable for μ_V and σ_W^2, therefore

$$\mu_V = \left(\frac{2\mu_{\overline{m}_v}}{\mu_{\overline{m}_v} + \mu_{\overline{m}'_v}}\right)^{\gamma} \exp\left(\mu_{\ln V} + \frac{1}{2}\sigma_{\ln V}^2\right) \tag{B.13}$$

where $\gamma = \dfrac{\upsilon_{\overline{m}'_v}}{\upsilon_{\overline{m}_v}}$ if $\upsilon_{\overline{m}_v} > \upsilon_{\overline{m}'_v}$ and $\gamma = \dfrac{\upsilon_{\overline{m}'_v} - \upsilon_{\overline{m}_v}}{\upsilon_{\overline{m}'_v}}$ if $\upsilon_{\overline{m}'_v} > \upsilon_{\overline{m}_v}$

$$\sigma_V^2 = \left(\frac{2\upsilon_{\overline{m}'_v}}{\upsilon_{\overline{m}_v} + \upsilon_{\overline{m}'_v}}\right)\mu_V^2\left[\exp\left(\sigma_{\ln V}^2\right) - 1\right] \tag{B.14}$$

In Eqs. (B.11–B.14), $\upsilon_{\bar{k}_h} = \sigma_{\bar{k}_h} / \mu_{\bar{k}_h}$ and $\upsilon_{\bar{k}'_h} = \sigma_{\bar{k}'_h} / \mu_{\bar{k}'_h}$ are the coefficients of variation of the equivalent permeability in the undisturbed and smear zones, respectively ($\sigma_{\bar{k}_h}$, $\mu_{\bar{k}_h}$, $\sigma_{\bar{k}'_h}$ and $\mu_{\bar{k}'_h}$ are the standard deviation and mean of $\bar{k}_h$ and $\bar{k}'_h$, respectively); $\upsilon_{\overline{m}_v} = \sigma_{\overline{m}_v} / \mu_{\overline{m}_v}$ and $\upsilon_{\overline{m}'_v} = \sigma_{\overline{m}'_v} / \mu_{\overline{m}'_v}$ are the coefficients of variation of the equivalent volume compressibility in the undisturbed and smear zones, respectively ($\sigma_{\overline{m}_v}$, $\mu_{\overline{m}_v}$, $\sigma_{\overline{m}'_v}$ and $\mu_{\overline{m}'_v}$ are the standard deviation and mean of $\overline{m}_v$ and $\overline{m}'_v$, respectively). With reference to Eqs. (4) and (5), and making use of Eqs. (19) and (21) lead to the following equations of the mean and standard deviation of $\bar{k}_h$ and $\bar{k}'_h$:

$$\mu_{\bar{k}_h} = \exp\left(\mu_{\ln \bar{k}_h} + \frac{1}{2}\sigma_{\ln \bar{k}_h}^2\right) = \exp\left(\ln \mu_{k_h} - \frac{1}{2}\ln\left(1 + \upsilon_{k_h}^2\right) + \frac{1}{2}\gamma\left(D_u\right)_{k_h}\ln\left(1 + \upsilon_{k_h}^2\right)\right) \tag{B.15}$$

$$\sigma_{\bar{k}_h} = \mu_{\bar{k}_h}\sqrt{\left[\exp\left(\sigma_{\ln \bar{k}_h}^2\right) - 1\right]} = \mu_{\bar{k}_h}\sqrt{\left[\exp\left(\gamma\left(D_u\right)_{k_h}\ln\left(1 + \upsilon_{k_h}^2\right)\right) - 1\right]} \tag{B.16}$$

$$\mu_{\bar{k}'_h} = \exp\left(\mu_{\ln \bar{k}'_h} + \frac{1}{2}\sigma_{\ln \bar{k}'_h}^2\right) = \exp\left(\ln \mu_{k'_h} - \frac{1}{2}\ln\left(1 + \upsilon_{k'_h}^2\right) + \frac{1}{2}\gamma\left(D_s\right)_{k'_h}\ln\left(1 + \upsilon_{k'_h}^2\right)\right) \tag{B.17}$$

$$\sigma_{\bar{k}'_h} = \mu_{\bar{k}'_h}\sqrt{\left[\exp\left(\sigma_{\ln \bar{k}'_h}^2\right) - 1\right]} = \mu_{\bar{k}'_h}\sqrt{\left[\exp\left(\gamma\left(D_s\right)_{k'_h}\ln\left(1 + \upsilon_{k'_h}^2\right)\right) - 1\right]} \tag{B.18}$$

Similarly, the mean and standard deviation of $\overline{m}_v$ and $\overline{m}'_v$ are thus:

$$\mu_{\overline{m}_v} = \exp\left(\ln \mu_{m_v} - \frac{1}{2}\ln\left(1+\upsilon_{m_v}^2\right) + \frac{1}{2}\gamma(D_u)_{m_v} \ln\left(1+\upsilon_{m_v}^2\right)\right) \tag{B.19}$$

$$\sigma_{\overline{m}_v} = \mu_{\overline{m}_v}\sqrt{\left[\exp\left(\gamma(D_u)_{m_v} \ln\left(1+\upsilon_{m_v}^2\right)\right)-1\right]} \tag{B.20}$$

$$\mu_{\overline{m}'_v} = \exp\left(\ln \mu_{m'_v} - \frac{1}{2}\ln\left(1+\upsilon_{m'_v}^2\right) + \frac{1}{2}\gamma(D_s)_{m'_v} \ln\left(1+\upsilon_{m'_v}^2\right)\right) \tag{B.21}$$

$$\sigma_{\overline{m}'_v} = \mu_{\overline{m}'_v}\sqrt{\left[\exp\left(\gamma(D_s)_{m'_v} \ln\left(1+\upsilon_{m'_v}^2\right)\right)-1\right]} \tag{B.22}$$

Substituting Eqs. (B.11) and (B.12) into Eqs. (B.3) and (B.5) lead to the following equations of $\mu_{\overline{\alpha}}$ and $\sigma_{\overline{\alpha}}^2$:

$$\mu_{\overline{\alpha}} = a + b\left(\frac{2\mu_{\bar{k}_h}}{\mu_{\bar{k}_h} + \mu_{\bar{k}'_h}}\right)^{\chi}\left(\exp\left(\mu_{\ln W} + \frac{1}{2}\sigma_{\ln W}^2\right)\right) \tag{B.23}$$

$$\sigma_{\overline{\alpha}}^2 = \left(\frac{2\upsilon_{\bar{k}'_h}}{\upsilon_{\bar{k}_h} + \upsilon_{\bar{k}'_h}}\right) b^2 \mu_W^2 \left[\exp\left(\sigma_{\ln W}^2\right)-1\right] \tag{B.24}$$

Again substituting Eqs. (B.13) and (B.14) into Eqs. (B.4) and (B.6) gives:

$$\mu_{\overline{\alpha}_{m_v}} = g + h\left(\frac{2\mu_{\overline{m}_v}}{\mu_{\overline{m}_v} + \mu_{\overline{m}'_v}}\right)^{\gamma}\left(\exp\left(\mu_{\ln V} + \frac{1}{2}\sigma_{\ln V}^2\right)\right) \tag{B.25}$$

$$\sigma_{\overline{\alpha}_{m_v}}^2 = \left(\frac{2\upsilon_{\overline{m}'_v}}{\upsilon_{\overline{m}_v} + \upsilon_{\overline{m}'_v}}\right) h^2 \mu_V^2 \left[\exp\left(\sigma_{\ln V}^2\right)-1\right] \tag{B.26}$$

Finally, the statistics (i.e., $\mu_{\ln\overline{\alpha}}$, $\sigma_{\ln\overline{\alpha}}^2$, $\mu_{\ln\overline{\alpha}_{m_v}}$ and $\sigma_{\ln\overline{\alpha}_{m_v}}^2$) of the underlying normally distributed $\ln\overline{\alpha}$ and $\ln\overline{\alpha}_{m_v}$ can be obtained from the obtained values of $\mu_{\overline{\alpha}}$, $\sigma_{\overline{\alpha}}^2$, $\mu_{\overline{\alpha}_{m_v}}$ and $\sigma_{\overline{\alpha}_{m_v}}^2$ by using Eqs. (2) and (3).

All six requested parameters (i.e., $\mu_{\ln\bar{k}_h}$, $\mu_{\ln\overline{m}_v}$, $\mu_{\ln\overline{\alpha}}$, $\mu_{\ln\overline{\alpha}_{m_v}}$, $\sigma_{\ln\overline{\alpha}}^2$ and $\sigma_{\ln\overline{\alpha}_{m_v}}^2$) are now known and can be used in Eqs. (42) and (43) for the estimation of $\mu_{\ln U^*(t)}$ and $\sigma_{\ln U^*(t)}^2$. Using the developed semi-analytical relationships, the procedure for calculating $\mu_{\ln U^*(t)}$ and $\sigma^2_{\ln U^*(t)}$ can be summarized as follows:

1. Determine all constant parameters involved in the RBSA–G2C1 (i.e., *C*, *a*, *b*, *g*, *h*, $\gamma(D_u)_{k_h}$, $\gamma(D_s)_{k'_h}$, $\gamma(D_u)_{m_v}$ and $\gamma(D_s)_{m'_v}$);
2. Calculate $\mu_{\ln \bar{k}_h}$ and $\mu_{\ln \overline{m}_v}$ from Eqs. (B.1) and (B.2);
3. Calculate $\mu_{\ln W}$, $\sigma^2_{\ln W}$, $\mu_{\ln V}$ and $\sigma^2_{\ln V}$ using Eqs. (B.7)-(B.10);
4. Calculate $\mu_{\bar{k}_h}$, $\sigma_{\bar{k}_h}$, $\mu_{\bar{k}'_h}$, $\sigma_{\bar{k}'_h}$, $\mu_{\overline{m}_v}$, $\sigma_{\overline{m}_v}$, $\mu_{\overline{m}'_v}$ and $\sigma_{\overline{m}'_v}$ using Eqs. (B.15)-(B.22), then determine $\upsilon_{\bar{k}_h}$, $\upsilon_{\bar{k}'_h}$, $\upsilon_{\overline{m}_v}$ and $\upsilon_{\overline{m}'_v}$;
5. Calculate μ_W and μ_V using Eqs. (B.11) and (B.13);
6. Using the values of $\mu_{\ln W}$, $\sigma^2_{\ln W}$, μ_W, $\mu_{\ln V}$, $\sigma^2_{\ln V}$, μ_V, $\upsilon_{\bar{k}_h}$, $\upsilon_{\bar{k}'_h}$, $\upsilon_{\overline{m}_v}$ and $\upsilon_{\overline{m}'_v}$ obtained in Steps 3-5, calculate $\mu_{\bar{\alpha}}$, $\sigma^2_{\bar{\alpha}}$, $\mu_{\bar{\alpha}_{m_v}}$ and $\sigma^2_{\bar{\alpha}_{m_v}}$ from Eqs. (B.23)-(B.26);
7. Use Eqs. (2) and (3) to determine $\sigma^2_{\ln \bar{\alpha}}$, $\mu_{\ln \bar{\alpha}}$, $\sigma^2_{\ln \bar{\alpha}_{m_v}}$ and $\mu_{\ln \bar{\alpha}_{m_v}}$ from the obtained values of $\mu_{\bar{\alpha}}$, $\sigma^2_{\bar{\alpha}}$, $\mu_{\bar{\alpha}_{m_v}}$ and $\sigma^2_{\bar{\alpha}_{m_v}}$ in Step 6; and
8. Evaluate $\mu_{\ln U^*(t)}$ and $\sigma^2_{\ln U^*(t)}$ by substituting $\mu_{\ln \bar{k}_h}$, $\mu_{\ln \overline{m}_v}$, $\mu_{\ln \bar{\alpha}}$ and $\mu_{\ln \bar{\alpha}_{m_v}}$ in Eq. (42), and $\sigma^2_{\ln \bar{\alpha}}$ and $\sigma^2_{\ln \bar{\alpha}_{m_v}}$ in Eq. (43).

Appendix C. RBSA model considering permeability as the only random variable

G1C2: *RBSA model considering k_h as continuous random variables over the entire unit cell and m_v deterministic*

The spatial variability of m_v is generally much less than that of k_h. Therefore, it is not unlikely to encounter soil with no or very little variability in m_v. For such condition, m_v can be considered as spatially constant without significantly affecting the final results. Treating k_h as spatially random and m_v as spatially constant, the C parameter in Eq. (23) is transformed to:

$$C = \frac{2t}{r_e^2 m_v \gamma_w \alpha \alpha_{m_v}} \tag{C.1}$$

The expressions for $\mu_{\ln U^*(t)}$ and $\sigma^2_{\ln U^*(t)}$ given in Eqs. (33) and (34) are then reduced to:

$$\mu_{\ln U^*(t)} = \ln C + \ln \mu_{k_h} - \frac{1}{2}\ln\left(1 + \upsilon^2_{k_h}\right) \tag{C.2}$$

$$\sigma^2_{\ln U^*(t)} = \gamma(D)_{k_h} \ln\left(1 + \upsilon^2_{k_h}\right) \tag{C.3}$$

G2C2: RBSA model considering k_h and k'_h as independent random variables and m_v deterministic

By considering k_h and k'_h as independent random variables and volume compressibility as spatially constant, the C parameter in Eq. (37) now becomes:

$$C = \frac{2t}{r_e^2 \gamma_w m_v \alpha_{m_v}} \tag{C.4}$$

The equations for $\mu_{\ln U^*(t)}$ and $\sigma^2_{\ln U^*(t)}$ given in Eqs. (42) and (43) are then reduced to:

$$\mu_{\ln U^*(t)} = \ln C + \mu_{\ln \bar{k}_h} - \mu_{\ln \bar{\alpha}} \tag{C.5}$$

$$\sigma^2_{\ln U^*(t)} = \sigma^2_{\ln \bar{\alpha}} \tag{C.6}$$

The three unknown parameters: $\mu_{\ln \bar{k}_h}$, $\mu_{\ln \bar{\alpha}}$ and $\sigma^2_{\ln \bar{\alpha}}$ in Eqs. (C.5) and (C.6) are already determined during the course of the development of the RBSA–G2C1 model as presented in Appendix B and can be readily used for estimation of $\mu_{\ln U^*(t)}$ and $\sigma^2_{\ln U^*(t)}$.

References

[1] Barron RA. Consolidation of fine-grained soils by drain wells. Transactions of the American Society of Civil Engineering 1948;113(718-54.

[2] Hansbo S. Consolidation of fine-grained soils by prefabricated drains. Proceedings of the 10th International Conference on Soil Mechanics and Foundation Engineering. Stockholm, Sweden; 1981. p. 677-82.

[3] Onoue A. Consolidation by vertical drains taking well resistance and smear into consideration. Soils and Foundations 1988;24(4):165-74.

[4] Chang CS. Uncertainty of one-dimensional consolidation analysis. Journal of Geotechnical Engineering 1985;111(12):1411-24.

[5] Freeze RA. Probabilistic one-dimensional consolidation. Journal of Geotechnical Engineering Division 1977;103(GT7):725-42.

[6] Huang J, Griffiths DV, Fenton GA. Probabilistic analysis of coupled soil consolidation. Journal of Geotechnical and Geoenvironmental Engineering 2010;136(3):417-30.

[7] Hong HP, Shang JQ. Probabilistic analysis of consolidation with prefabricated vertical drains for soil improvement. Canadian Geotechnical Journal 1998;35(4):666-77.

[8] Zhou W, Hong HP, Shang JQ. Probabilistic design method of prefabricated vertical drains for soil improvement. Journal of Geotechnical and Geoenvironmental Engineering 1999;125(8):659-64.

[9] Walker RT, Indraratna B. Vertical drain consolidation with parabolic distribution of permeability in smear zone. Journal of Geotechnical and Geoenvironmental Engineering 2006;132(7):937-41.

[10] Basu D, Basu P, Prezzi M. Analytical solutions for consolidation aided by vertical drains. Geomechanics and Geoengineering: An International Journal 2006;1(1):63-71.

[11] Fenton G, Griffiths DV. Probabilistic foundation settlement on spatially random soil. Journal of Geotechnical and Geoenvironmental Engineering 2002;128(5):381-90.

[12] Griffiths DV, Fenton GA. Probabilistic settlement analysis by stochastic and random finite-element methods. Journal of geotechnical and geoenvironmental engineering 2009;135(11):1629-37.

[13] Fenton GA, Vanmarcke EH. Simulation of random fields via local average subdivision. Journal of Engineering Mechanics 1990;116(8):1733-49.

[14] Pyrah IC. One-dimensional consolidation of layered soils. Geotechnique 1996;46(3):555-60.

[15] Vanmarcke EH. Random fields: analysis and synthesis. Massachusetts: The MIT Press, 1984.

[16] Griffiths DV, Fenton GA. Seepage beneath water retaining structures founded on spatially random soil. Géotechnique 1993;43(4):577-87.

[17] Fenton GA, Griffiths DV. Risk assessment in geotechnical engineering. New Jersey: John Wiley and Sons, 2008.

[18] Lloret-Cabot M, Fenton GA, Hicks MA. On the estimation of scale of fluctuation in geostatistics. Georisk 2014;8(2):129-40.

[19] Smith IM, Griffiths DV. Programming the finite element method. 4th ed. Chichester, West Sussex: John Wiley and Sons, 2004.

[20] Ching J, Phoon K-K. Effect of element sizes in random field finite element simulations of soil shear strength. Computers & structures 2013;126(1):120-34.

[21] Harada T, Shinozuka M. The scale of correlation for stochastic fields. New York: Department of Civil Engineering and Engineering Mechanics, Columbia University, 1986.

[22] Sharma JS, Xiao D. Characterization of a smear zone around vertical drains by large-scale laboratory tests. Canadian Geotechical Journal 2000;37(6):1265-71.

[23] Chu J, Bo MW, Choa V. Practical considerations for using vertical drains in soil improvement projects. Geotextiles and Geomembranes 2004;22(1-2):101-17.

[24] Walker RT. Analytical solutions for modeling soft soil consolidation by vertical drains. Wollongong, Australia: Thesis (PhD). University of Wollongong, 2006.

[25] Beacher GB, Christian JT. Reliability and Statistics in Geotechnical Engineering. Chichester, England: John Wiley & Sons, 2003.

[26] Phoon KK, Kulhawy FH. Characterisation of geotechnical variability. Canadian Geotechnical Journal 1999;36(4):612-24.

[27] Bari MW, Shahin MA, Soubra A-H. Single vs multi-drain analyses of probabilistic soil consolidation via prefabricated vertical drains. 12th International Conference on Applications of Statistics and Probability in Civil Engineering. Vancouver, Canada; 2015 (accepted).

[28] Rixner JJ, Kraemer SR, Smith AD. Prefabricated vertical drains, Vol. I: Engineering guidelines. Washington D. C.: Federal Highway Administration, 1986.

[29] Benjamin JR, Cornell CA. Probability, statistics, and decision for civil engineers. New York: McGraw-Hill, 1970.

Figure Captions:

Fig. 1. Schematic diagram of soil consolidation with prefabricated vertical drain: (a) cylindrical unit cell; (b) equivalent square geometry with FE mesh discretization

Fig. 2. Comparison between FEMC and RBSA–G1C1 for the effect of: (a) υ on $\mu_{\ln U^*}$ for θ = 0.5m (b) θ on $\mu_{\ln U^*}$ for υ_{k_h} = 200%, υ_{m_v} = 20% (c) υ on $\sigma_{\ln U^*}$ for θ = 0.5m and (d) θ on $\sigma_{\ln U^*}$ for υ_{k_h} = 200%, υ_{m_v} = 20%

Fig. 3. Comparison between FEMC and RBSA–G1C1 for the effect of: (a) υ on $P[U \geq U_{90}]$ for θ = 0.5m (b) θ on $P[U \geq U_{90}]$ for υ_{k_h} = 200%, υ_{m_v} = 20%

Fig. 4. Comparison between FEMC and RBSA–G2C1 for the effect of: (a) υ_u on $\mu_{\ln U^*}$ at fixed value of $\upsilon_{k'_h}$ = 100%, $\upsilon_{m'_v}$ = 10%, $\theta_u = \theta_s$ = 1.0m; (b) υ_s on $\mu_{\ln U^*}$ at fixed value of υ_{k_h} = 100%, υ_{m_v} = 10%, $\theta_u = \theta_s$ = 1.0m

Fig. 5. Comparison between FEMC and RBSA–G2C1 for the effect of: (a) θ_u on $\mu_{\ln U^*}$ at fixed value of $\upsilon_{k_k} = \upsilon_{k'_h}$ = 200%, $\upsilon_{m_v} = \upsilon_{m'_v}$ = 20%, θ_s = 0.25m; (b) θ_s on $\mu_{\ln U^*}$ at fixed value of υ_{k_k} = $\upsilon_{k'_h}$ = 200%, $\upsilon_{m_v} = \upsilon_{m'_v}$ = 20%, θ_u = 0.25m

Fig. 6. Comparison between FEMC and RBSA–G2C1 for the effect of: (a) υ_u on $\sigma_{\ln U^*}$ at fixed value of $\upsilon_{k'_h}$ = 100%, $\upsilon_{m'_v}$ = 10%, $\theta_u = \theta_s$ = 1.0m; (b) υ_s on $\sigma_{\ln U^*}$ at fixed value of υ_{k_h} = 100%, υ_{m_v} = 10%, $\theta_u = \theta_s$ = 1.0m

Fig. 7. Comparison between FEMC and RBSA–G2C1 for the effect of: (a) θ_u on $\sigma_{\ln U^*}$ at fixed value of $\upsilon_{k_k} = \upsilon_{k'_h}$ = 200%, $\upsilon_{m_v} = \upsilon_{m'_v}$ = 20%, θ_s = 0.25m; (b) θ_s on $\sigma_{\ln U^*}$ at fixed value $\upsilon_{k_k} = \upsilon_{k'_h}$ = 200%, $\upsilon_{m_v} = \upsilon_{m'_v}$ = 20%, θ_u = 0.25m

Fig. 8. Comparison between FEMC and RBSA–G2C1 for the effect of: (a) υ_u on $P[U \geq U_{90}]$ at fixed value of $\upsilon_{k'_h}$ = 100%, $\upsilon_{m'_v}$ = 10%, $\theta_u = \theta_s$ = 1.0m; (b) υ_s on $P[U \geq U_{90}]$ at fixed value of υ_{k_h} = 100%, υ_{m_v} = 10%, $\theta_u = \theta_s$ = 1.0m

Fig. 9. Comparison between FEMC and RBSA–G2C1 for the effect of: (a) θ_u on $P[U \geq U_{90}]$ at fixed value of $\upsilon_{k_k} = \upsilon_{k'_h}$ = 200%, $\upsilon_{m_v} = \upsilon_{m'_v}$ = 20%, θ_s = 0.25m (b) θ_s on $P[U \geq U_{90}]$ at fixed value $\upsilon_{k_k} = \upsilon_{k'_h}$ = 200%, $\upsilon_{m_v} = \upsilon_{m'_v}$ = 20%, θ_u = 0.25m

Fig. 10. Comparison between (a) $\mu_{\ln U^*}$ (b) $\sigma_{\ln U^*}$ and (c) $P[U \geq U_{90}]$ obtained from FEMC and RBSA methods for a unit cell having L/S = 5 and anisotropic θ

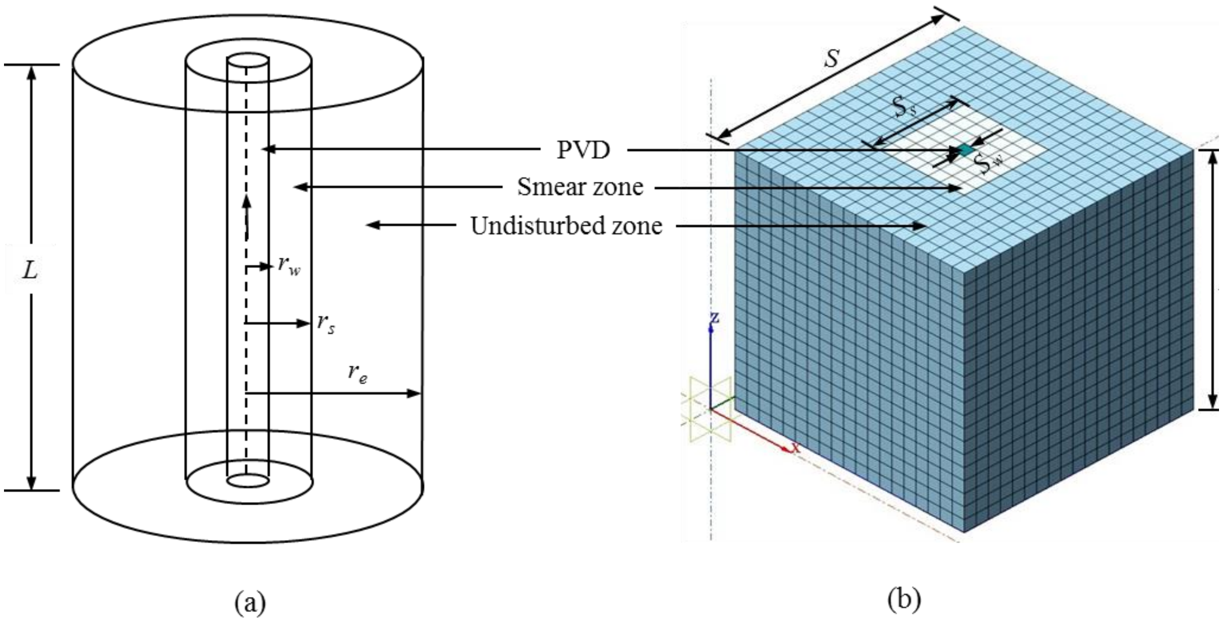

Fig. 1. Schematic diagram of soil consolidation with prefabricated vertical drain: (a) cylindrical unit cell; (b) equivalent square geometry with FE mesh discretization

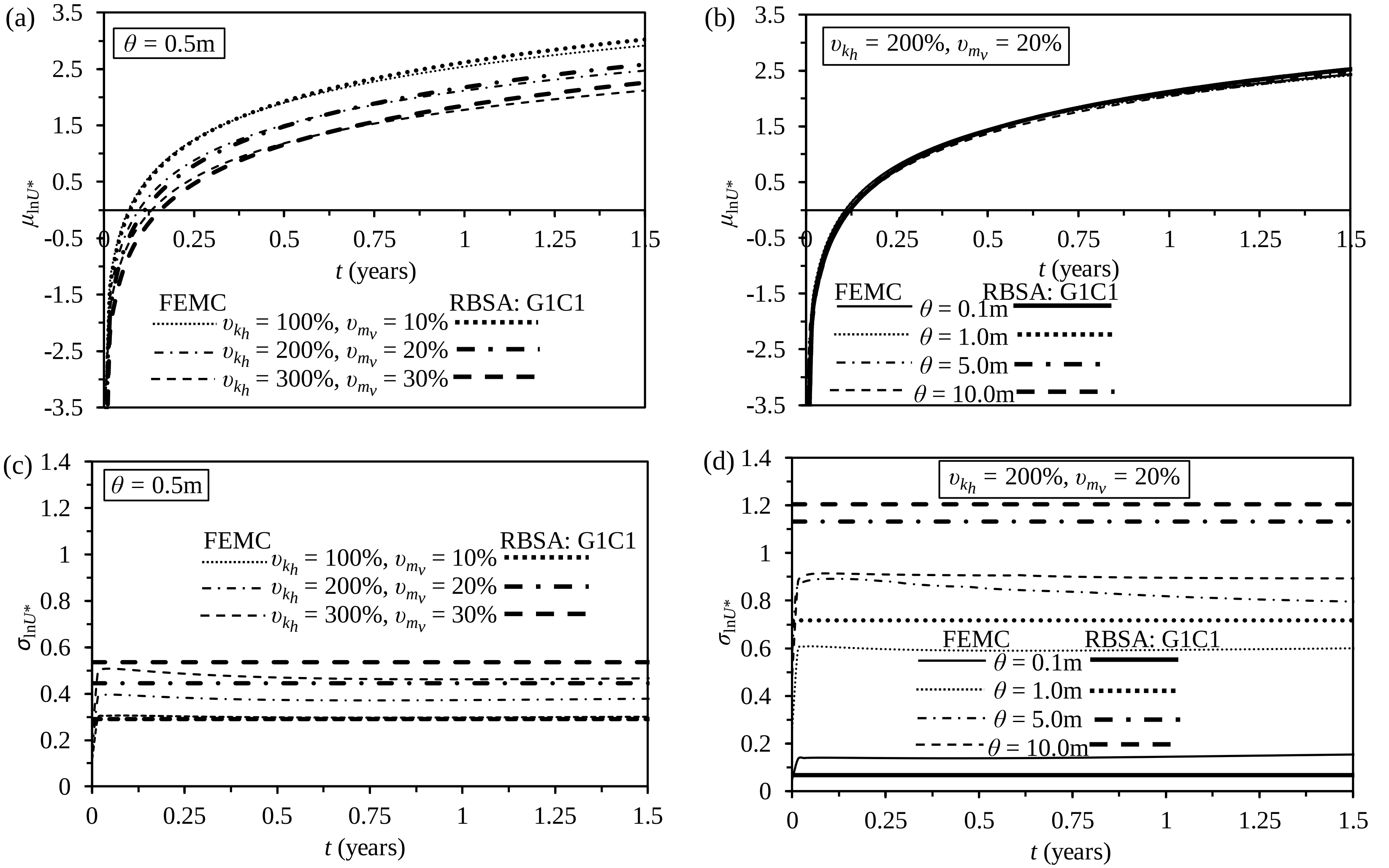

Fig. 2. Comparison between FEMC and RBSA–G1C1 for the effect of: (a) υ on $\mu_{\ln U^*}$ for θ = 0.5m (b) θ on $\mu_{\ln U^*}$ for υ_{k_h} = 200%, υ_{m_v} = 20% (c) υ on $\sigma_{\ln U^*}$ for θ = 0.5m and (d) θ on $\sigma_{\ln U^*}$ for υ_{k_h} = 200%, υ_{m_v} = 20%

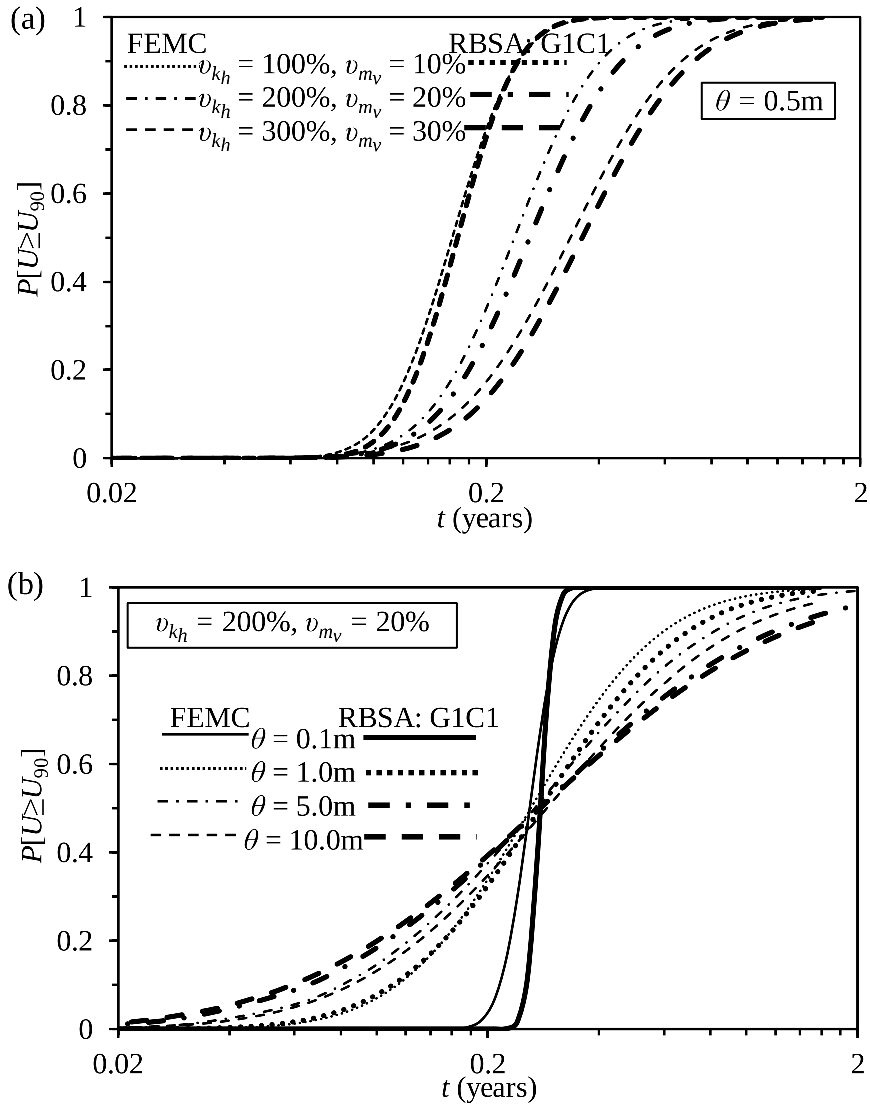

Fig. 3. Comparison between FEMC and RBSA–G1C1 for the effect of: (a) υ on $P[U \geq U_{90}]$ for θ = 0.5m (b) θ on $P[U \geq U_{90}]$ for υ_{k_h} = 200%, υ_{m_v} = 20%

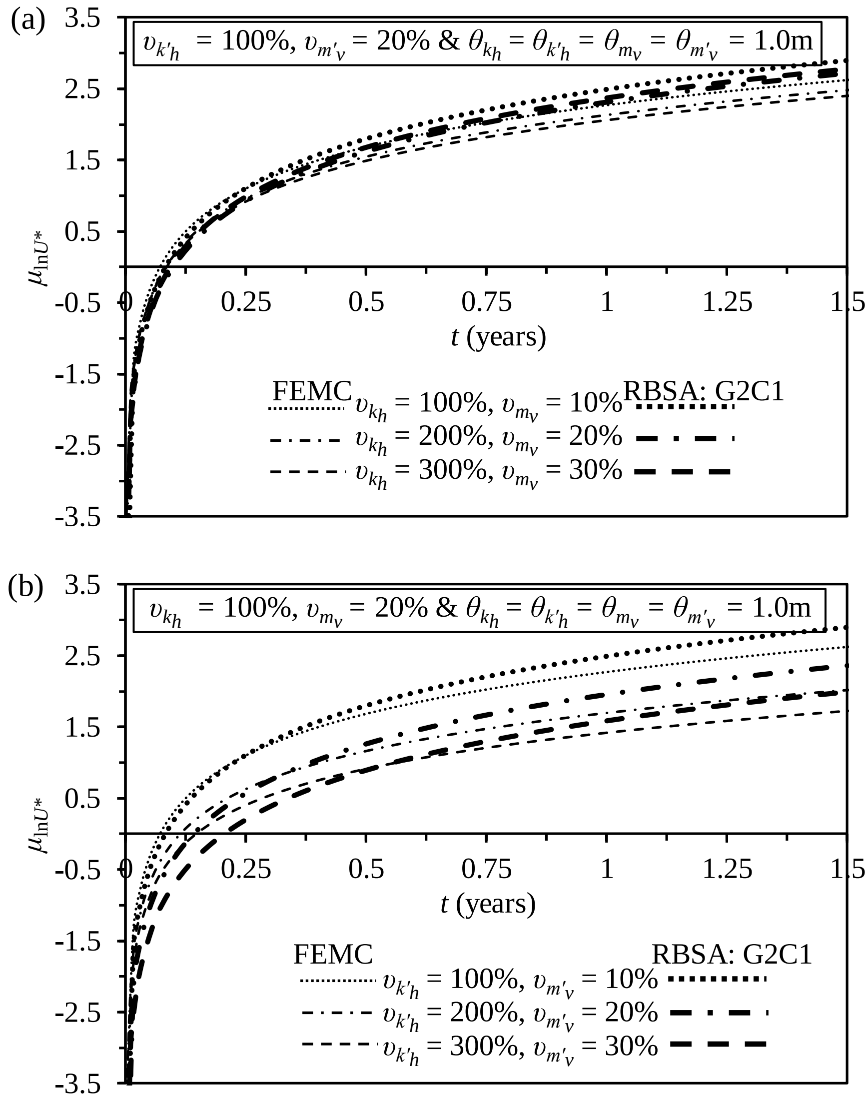

Fig. 4. Comparison between FEMC and RBSA–G2C1 for the effect of: (a) υ_u on $\mu_{\ln U^*}$ at fixed value of $\upsilon_{k'_h}$ = 100%, $\upsilon_{m'_v}$ = 10%, $\theta_u = \theta_s$ = 1.0m; (b) υ_s on $\mu_{\ln U^*}$ at fixed value of υ_{k_h} = 100%, υ_{m_v} = 10%, $\theta_u = \theta_s$ = 1.0m

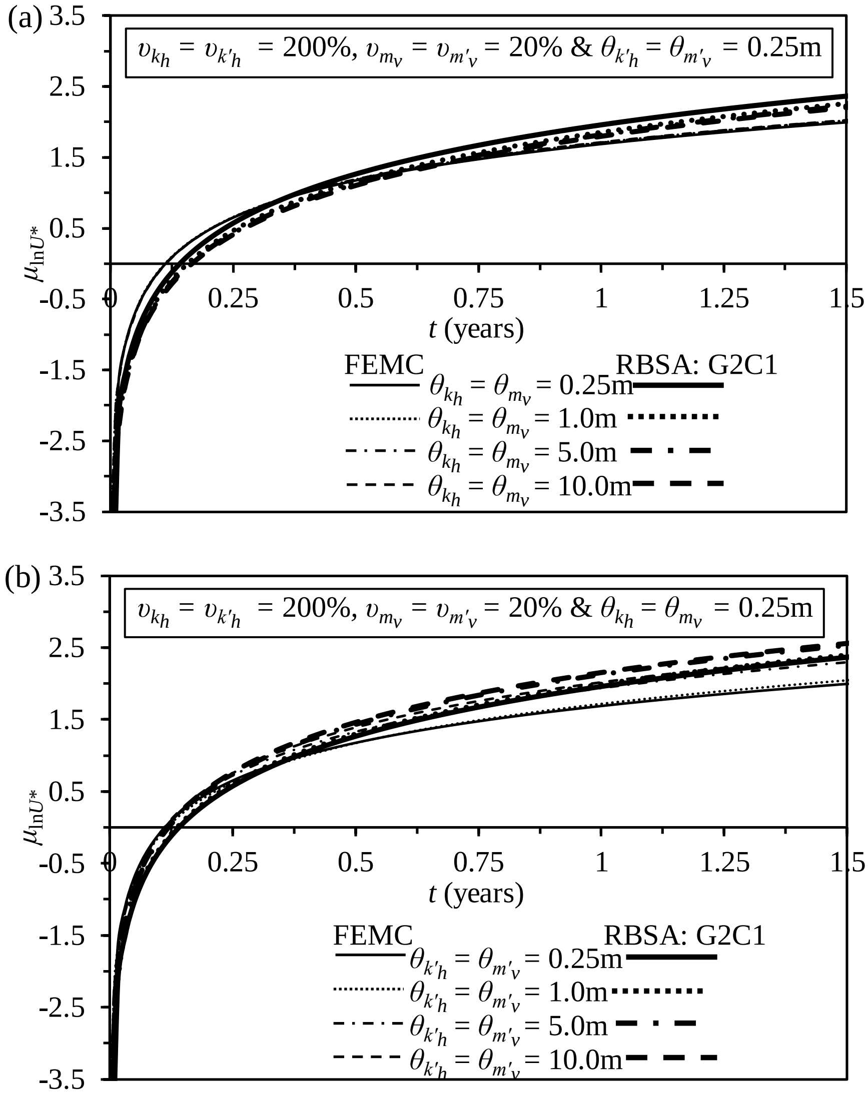

Fig. 5. Comparison between FEMC and RBSA–G2C1 for the effect of: (a) θ_u on $\mu_{\ln U^*}$ at fixed value of $\upsilon_{k_k} = \upsilon_{k'_h}$ = 200%, $\upsilon_{m_v} = \upsilon_{m'_v}$ = 20%, θ_s = 0.25m; (b) θ_s on $\mu_{\ln U^*}$ at fixed value of $\upsilon_{k_k} = \upsilon_{k'_h}$ = 200%, $\upsilon_{m_v} = \upsilon_{m'_v}$ = 20%, θ_u = 0.25m

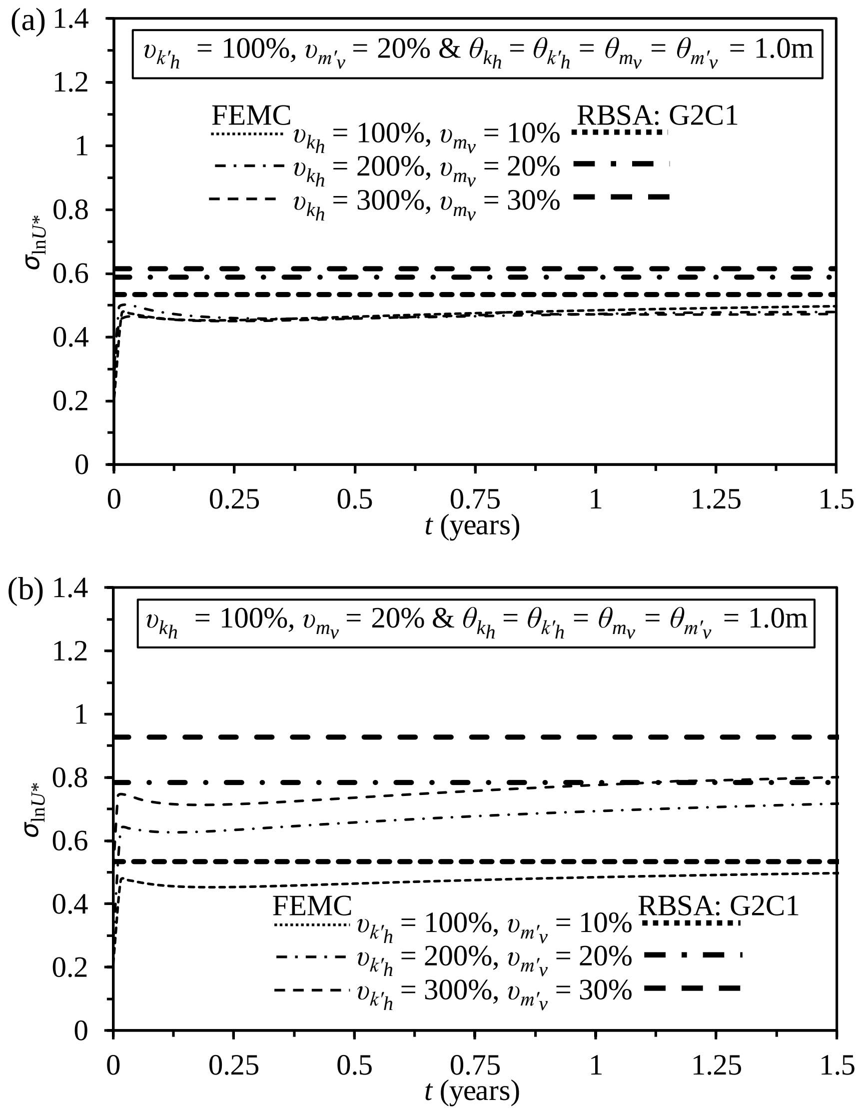

Fig. 6. Comparison between FEMC and RBSA–G2C1 for the effect of: (a) υ_u on $\sigma_{\ln U^*}$ at fixed value of $\upsilon_{k'_h}$ = 100%, $\upsilon_{m'_v}$ = 10%, $\theta_u = \theta_s$ = 1.0m; (b) υ_s on $\sigma_{\ln U^*}$ at fixed value of υ_{k_h} = 100%, υ_{m_v} = 10%, $\theta_u = \theta_s$ = 1.0m

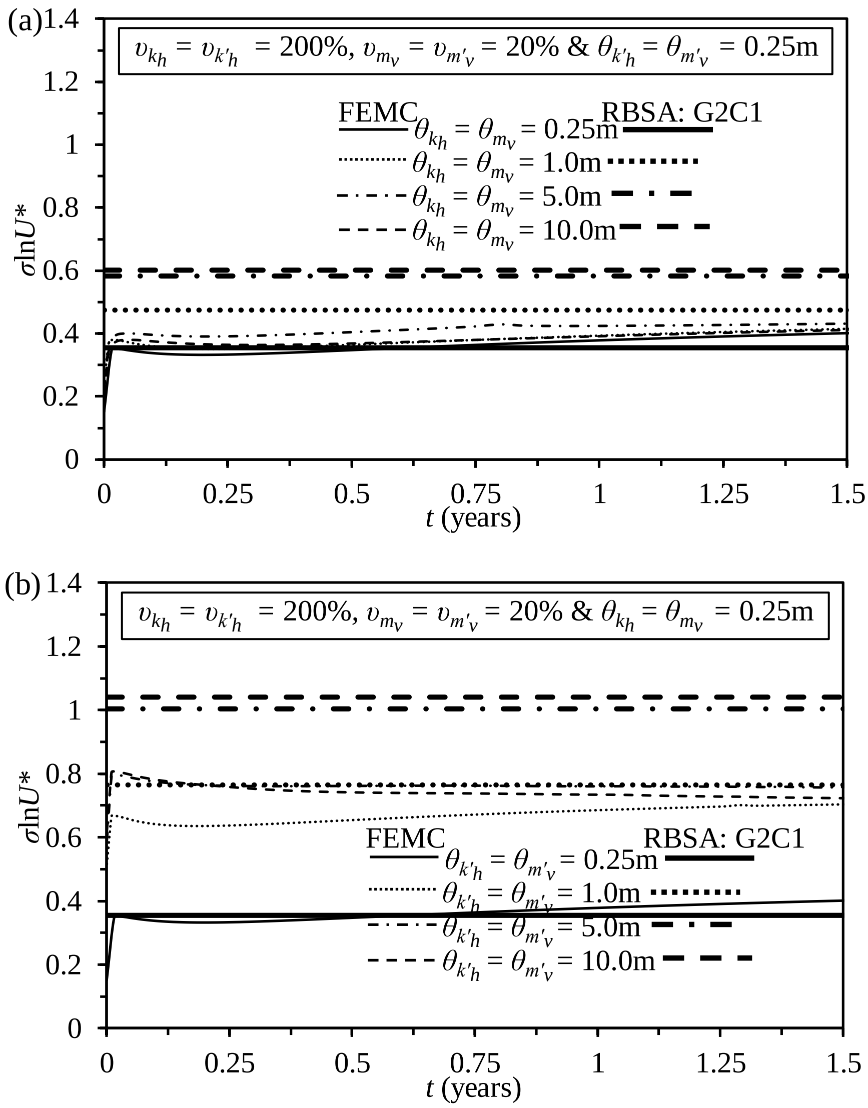

Fig. 7. Comparison between FEMC and RBSA–G2C1 for the effect of: (a) θ_u on $\sigma_{\ln U^*}$ at fixed value of $\upsilon_{k_k} = \upsilon_{k'_h}$ = 200%, $\upsilon_{m_v} = \upsilon_{m'_v}$ = 20%, θ_s = 0.25m; (b) θ_s on $\sigma_{\ln U^*}$ at fixed value $\upsilon_{k_k} = \upsilon_{k'_h}$ = 200%, $\upsilon_{m_v} = \upsilon_{m'_v}$ = 20%, θ_u = 0.25m

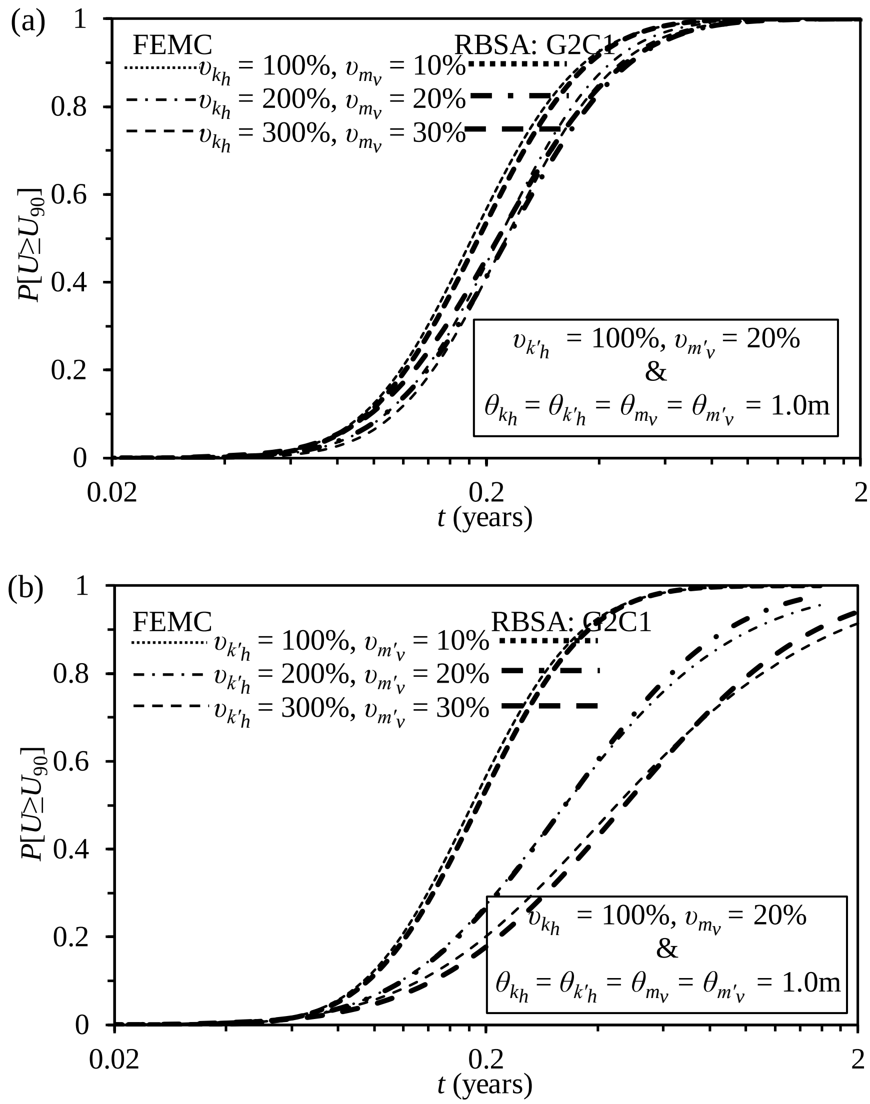

Fig. 8. Comparison between FEMC and RBSA–G2C1 for the effect of: (a) υ_u on $P[U \geq U_{90}]$ at fixed value of $\upsilon_{k'_h}$ = 100%, $\upsilon_{m'_v}$ = 10%, $\theta_u = \theta_s$ = 1.0m; (b) υ_s on $P[U \geq U_{90}]$ at fixed value of υ_{k_h} = 100%, υ_{m_v} = 10%, $\theta_u = \theta_s$ = 1.0m

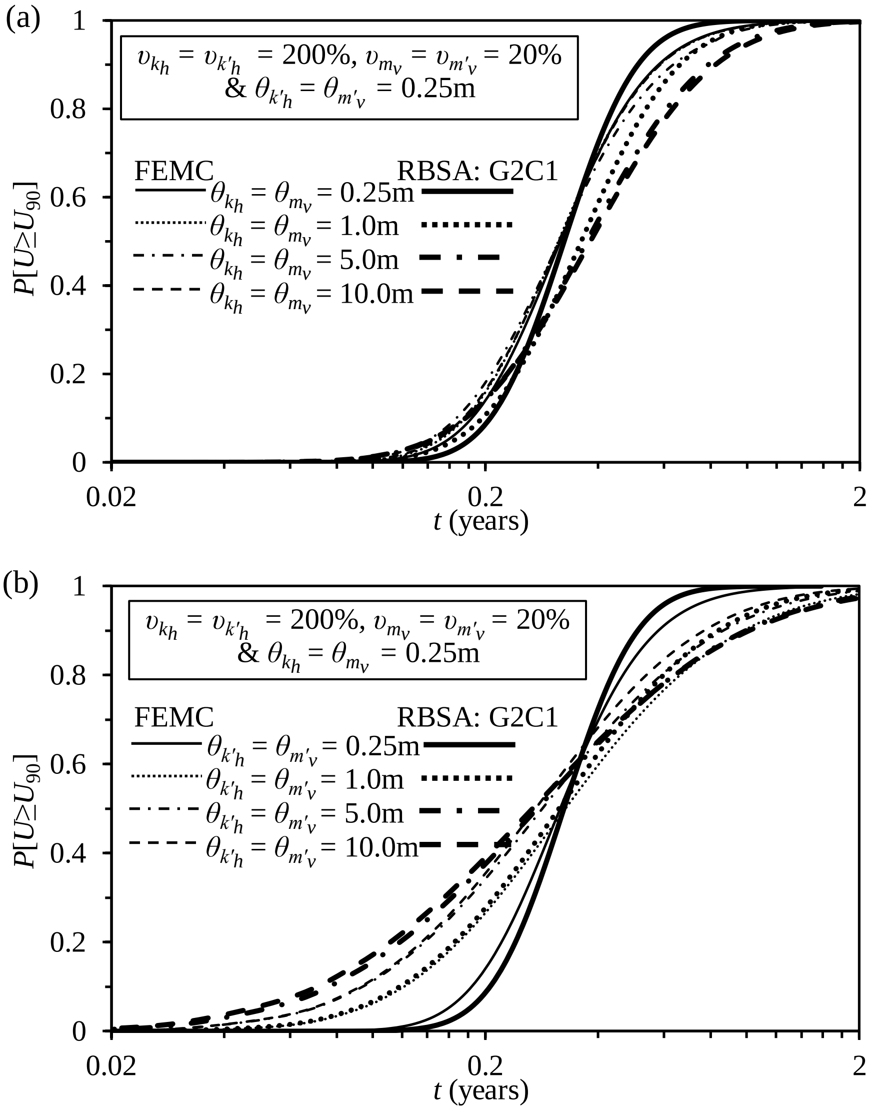

Fig. 9. Comparison between FEMC and RBSA–G2C1 for the effect of: (a) θ_u on $P[U \geq U_{90}]$ at fixed value of $\upsilon_{k_k} = \upsilon_{k'_h}$ = 200%, $\upsilon_{m_v} = \upsilon_{m'_v}$ = 20%, θ_s = 0.25m (b) θ_s on $P[U \geq U_{90}]$ at fixed value $\upsilon_{k_k} = \upsilon_{k'_h}$ = 200%, $\upsilon_{m_v} = \upsilon_{m'_v}$ = 20%, θ_u = 0.25m

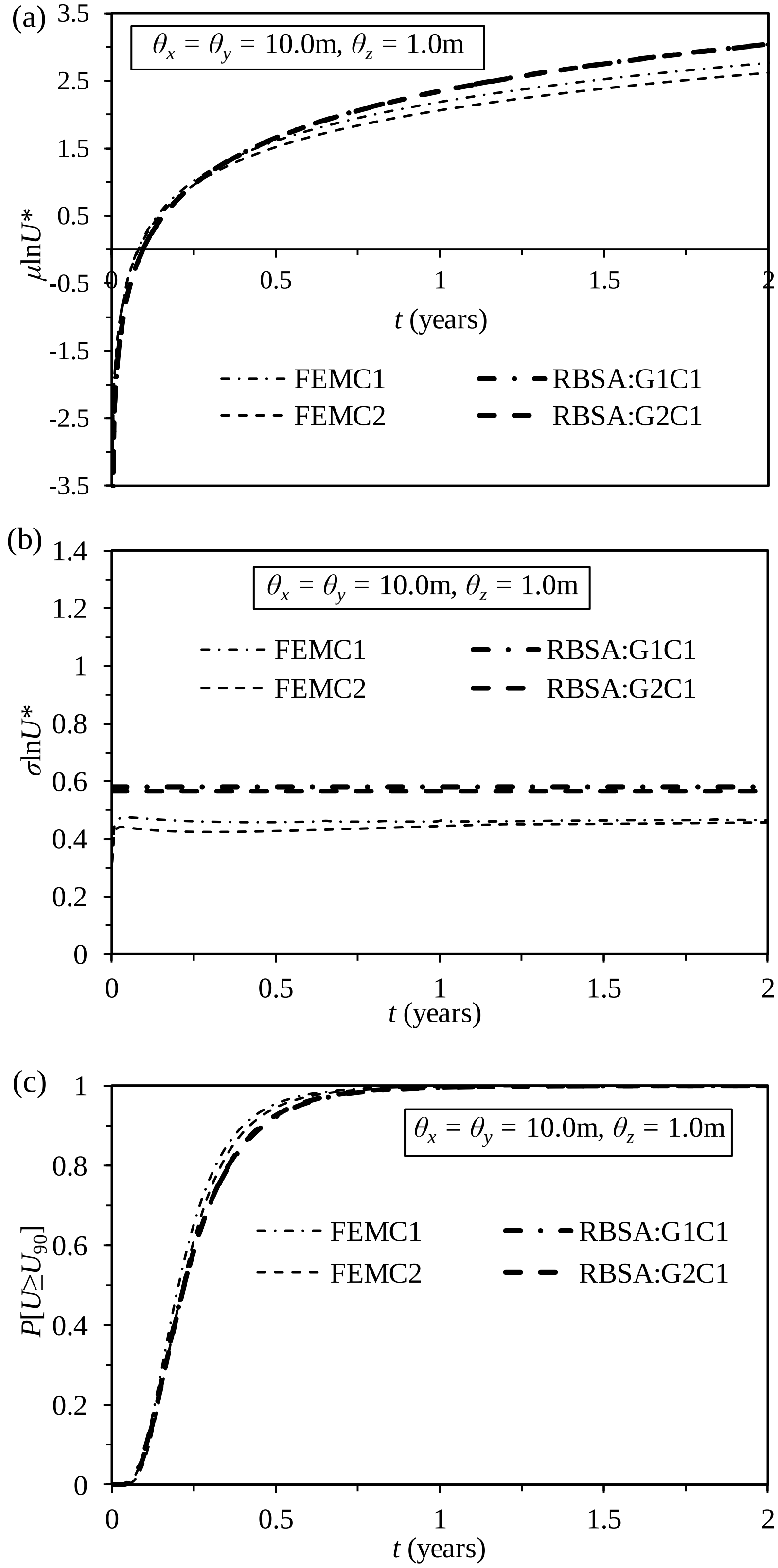

Fig. 10. Comparison between (a) $\mu_{\ln U*}$ (b) $\sigma_{\ln U*}$ and (c) $P[U \geq U_{90}]$ obtained from FEMC and RBSA methods for unit cell having L/S = 5 and anisotropic θ

1046

1047